Continuous Time System Level Synthesis for Mixed $\mathcal{H}_2/\mathcal{H}_\infty$ Control Design Using Simple Pole Approximation

Zhong Fang and Michael W. Fisher

***Abstract*—Design of mixed $\mathcal{H}_2/\mathcal{H}_\infty$ optimal linear feedback controllers is a challenging but important problem in many applications. The main difficulties stem from nonconvexity and infinite dimensionality of the associated optimization problem for the design. System level synthesis (SLS) tackles nonconvexity by reparameterizing the variables to transform the design into a convex optimization problem. SLS has several advantages over traditional convex reparameterization approaches, such as the ability to easily impose structural constraints on the closed-loop system responses with a convex formulation. While SLS has been successfully applied in discrete time, and the basic theory has been extended to continuous time, no tractable method currently exists for continuous time mixed $\mathcal{H}_2/\mathcal{H}_\infty$ control design using SLS. Part of the challenge has been that traditional finite dimensional approximation methods, such as finite impulse response approximation, lead to numerical ill-conditioning or even closed-loop instability. In this work, the first practical and tractable continuous time mixed $\mathcal{H}_2/\mathcal{H}_\infty$ control design based on SLS is developed. To do so, a novel Galerkin-type method for finite dimensional approximations of transfer functions in continuous time Hardy space is introduced based on transfer functions with a selection of simple poles. Approximation error bounds are established for the first time for this simple pole approximation (SPA) in continuous time. These bound the error based on the geometry of the pole selection, and show that under very mild conditions, this error goes to zero as the number of approximating poles approaches infinity. After combining the SPA with SLS, the KYP lemma is used to evaluate the $\mathcal{H}_2$ and $\mathcal{H}_\infty$ norms using linear matrix inequalities, resulting in a convex semidefinite program for the control design. The approximation error bounds for SPA are then used to develop suboptimality bounds for this novel control design method that guarantee convergence to the ground-truth global optimum under mild conditions. These suboptimality bounds are then specialized to derive a convergence rate for a particularly interesting pole selection over a trapezoid. Finally, the excellent performance of the proposed method is illustrated on an example of power converter control design.**

***Index Terms*—$\mathcal{H}_2$ and $\mathcal{H}_\infty$ control, optimal control, system level synthesis.**

I. Introduction

Mixed $\mathcal{H}_2/\mathcal{H}_\infty$ optimal linear feedback control design in continuous time is a valuable problem, enabling an explicit trade-off between performance and robustness, and has a long history [1]. However, it remains challenging to solve efficiently as methods for $\mathcal{H}_2$ or $\mathcal{H}_\infty$ design alone [2] do not directly yield optimal solutions to mixed $\mathcal{H}_2/\mathcal{H}_\infty$ design. The first major difficulty is that the design problem is nonconvex. Convex reparameterization, which involves a change of variables and to render the optimization problem convex [3], is one approach to address this. A classical example is the Youla parametrization [4], while more recent methods include system level synthesis (SLS) [5] and input output parametrization (IOP) [6]. For this work we are interested in state feedback design, whereas IOP is restricted to output feedback, and therefore focus on SLS. SLS has several advantages over Youla parameterization, as detailed in [2], [3], [7]–[10], which include directly parameterizing via the closed-loop system responses, not requiring coprime decomposition, and facilitating structural design specifications. However, SLS requires the incorporation of additional affine constraints into the design problem.

Convex reparameterizations result in a convex yet infinite dimensional design problem because the decision variables lie in an infinite dimensional Hardy space. Hence, the design problem is in general still intractable in this form. Different finite dimensional approximation methods, such as finite impulse response (FIR) [5] and simple pole approximation (SPA) [11], have been combined with SLS to obtain tractable control design methods for mixed $\mathcal{H}_2/\mathcal{H}_\infty$ design in discrete time [5], [12], [13], but no tractable methods for mixed $\mathcal{H}_2/\mathcal{H}_\infty$ design in continuous time using SLS have been developed. One of the main challenges for the continuous time setting is that traditional finite dimensional approximation methods, such as FIR, fail to provide a tractable design method in continuous time because they result in closed-loop instability and/or numerical ill-conditioning [2], [14]. In contrast, the approximation method SPA that was recently introduced in our prior work for the discrete time setting [11] offers the potential for a tractable design method in continuous time, but SPA has not been developed in continuous time yet. The goal of the present paper is to develop the first tractable method for mixed $\mathcal{H}_2/\mathcal{H}_\infty$ control design in continuous time using SLS.

To do so, the first key contribution of the present paper is the development of SPA in continuous time. Bounds on the approximation error between any transfer function in continuous time Hardy space and the SPA are derived which are proportional to the geometric distance between the poles of that transfer function and the poles of the SPA. Combining these approximation error bounds with the notion of a space-filling sequence of poles and considering a SPA with poles selected from any arbitrary compact set in the left half plane, it is shown that SPA converges to any transfer function whose

Z. Fang and M. W. Fisher are with the Department of Electrical and Computer Engineering, University of Waterloo, Waterloo, Ontario, Canada (e-mail: {z4fang, michael.fisher}@uwaterloo.ca).

poles lie in this compact set at a uniform convergence rate that depends purely on the geometry of the pole selection.

To develop a tractable mixed $\mathcal{H}_2/\mathcal{H}_\infty$ control design method in continuous time using SLS with SPA, the key idea is to use the KYP lemma to express the $\mathcal{H}_2$ and $\mathcal{H}_\infty$ norms as linear matrix inequalities (LMIs). To do so, we first find novel closed-loop state space realizations that are carefully chosen to ensure that these norms can be expressed as convex LMIs rather than nonconvex bilinear matrix inequalities (BMIs). However, transforming the affine constraints required for SLS to state space renders them nonconvex. Therefore, we propose a hybrid design in which the $\mathcal{H}_2$ and $\mathcal{H}_\infty$ norms are expressed via LMIs with state space realizations, while the SLS constraints are retained in the frequency domain to preserve their affine structure. This results in a convex semidefinite program (SDP) for the control design that can be solved efficiently, and is the first tractable method for mixed $\mathcal{H}_2/\mathcal{H}_\infty$ control synthesis in continuous time using SLS.

The SPA approximation error bounds are then leveraged to develop suboptimality bounds for the proposed design method that show convergence of SPA to the ground-truth optimal solution of the infinite dimensional problem as the number of poles in the approximation diverges. A uniform convergence rate is provided for these suboptimality bounds that depends purely on the geometry of the pole selection. Finally, a particularly interesting space-filling sequence of poles is proposed in which poles are selected from the intersection of a grid with a trapezoid in the left half plane. An example of power converter control design for providing frequency and voltage regulation to the power grid shows the efficiency and excellent performance of SLS with SPA in continuous time.

The development of the approximation error bounds for SPA, and the suboptimality bounds for SLS with SPA, in continuous time is not merely a straightforward application of analogous arguments from discrete time SPA because of the following challenges in continuous time: i) the set of stable poles is bounded in the discrete time unit disk, but unbounded in the continuous time left half plane, ii) the noncompactness of the domain (the imaginary axis) over which the $\mathcal{H}_2$ and $\mathcal{H}_\infty$ norms are calculated as opposed to the compact unit circle in discrete time, iii) in discrete time the $\mathcal{H}_2$ norm can be upper bounded by a constant multiple of the $\mathcal{H}_\infty$ norm, but this is not possible in continuous time. These challenges require the development of new methods to establish the desired bounds that were not required for the discrete time setting.

Continuous time SPA and its associated approximation error bounds are developed in generality in this paper before being applied to SLS. As a result, it has the potential to be applied to a range of other continuous time control design techniques, including IOP and SLS with output feedback, to develop novel tractable control design methods. Furthermore, the approach used to derive suboptimality bounds in the present paper may serve as a general methodology for establishing similar guarantees in these settings.

The rest of this paper is structured as follows. Section II provides some notation. The problem formulation and a review of SLS are presented in Section III. Section IV provides the main results, including the continuous time SPA and approximation error bounds, as well as the continuous time SLS with SPA control design method and suboptimality bounds. A valuable state space realization of the closed-loop system and the derivation of the control design method are presented in Section V. Section VI shows a numerical example. Section VII gives the proofs of the theoretical results. Finally, Section VIII concludes this article.

II. Notation

We will use the following notation throughout the article. Let $\mathbb{C}^-$ be the open left half plane. For a matrix M, let $M^\intercal$, M^*, and $\mathrm{Tr}\{M\}$ denote its transpose, conjugate transpose, and trace, respectively. For a complex number s, let $\mathrm{Re}(s)$, $\mathrm{Im}(s)$, and $\overline{s}$ represent the real part, imaginary part, and complex conjugate of s, respectively. Let $s = \mathrm{Re}(s) + j\mathrm{Im}(s) =: s_x + js_y$. For any matrix A, its spectral and Frobenius norm are denoted by $\|A\|_2 = \sigma_{\max}(A)$ (the largest singular value of A), $\|A\|_F = \sqrt{A^\intercal A}$ respectively. We say a matrix A is Hurwitz if all of its eigenvalues lie in the open left half plane. A positive definite matrix P is denoted by $P \succ 0$. The set of complex matrices of dimension $n \times m$ is denoted by $\mathbb{C}^{n\times m}$. The sets of real and symmetric matrices of dimension $n \times m$ and $n \times n$ are denoted by $\mathbb{R}^{n\times m}$ and $\mathbb{S}^n$, respectively. 0^n and I^n are the $n \times n$ zero and identity matrices, and n is often omitted if there is no ambiguity. We define the floor function $\lfloor x \rfloor := \max\{n \in \mathbb{Z} : n \leq x\}$ for any $x \in \mathbb{R}$. We use calligraphic letters such as $\mathcal{S}$ to denote sets, let $|\mathcal{S}|$ be its cardinality (i.e., the number of elements it contains). Let $\mathcal{M}$ denote a collection of matrices of scalars $\{M_i\}_{i=1}^l$, define the block diagonal concatenation operator by $D(\mathcal{M}) := \begin{bmatrix} M_1 & & \\ & \ddots & \\ & & M_l \end{bmatrix}$ where the off-diagonal entries are all zero, and define the block row concatenation operator by $R(\mathcal{M}) := \begin{bmatrix} M_1 & \cdots & M_l \end{bmatrix}$. The operator $\otimes$ denotes the Kronecker product between any two matrices. Let m and n be nonnegative integers, $m!$ denote the standard factorial, and $m!!$ denote double factorial by $m!! = \prod_{k=0}^{\lfloor (m-1)/2 \rfloor}(m-2k)$.

We denote the set of real, rational, proper, and stable transfer function matrices as $\mathcal{RH}_\infty$, and the subset of $\mathcal{RH}_\infty$ that are strictly proper as $\frac{1}{s}\mathcal{RH}_\infty$. For $S \in \mathcal{RH}_\infty$, define the norms $\|S\|_{\mathcal{H}_\infty} = \sup_{\omega\in\mathbb{R}} \sigma_{\max}(S(j\omega))$ and $\|S\|_{\mathcal{H}_2}^2 = \frac{1}{2\pi}\mathrm{Tr}\int_{-\infty}^{\infty} S(j\omega)^* S(j\omega)\,\mathrm{d}\omega$.

III. Preliminaries

A. Problem Formulation

Consider the LTI system in continuous time described by the following state space representation:

$$\begin{aligned} x(k+1) &= Ax(k) + Bu(k) + \hat{B}w(k) \\ y(k) &= Cx(k) \end{aligned} \tag{1}$$

where $x(k) \in \mathbb{R}^n$, $u(k) \in \mathbb{R}^p$, $w(k) \in \mathbb{R}^q$, $y(k) \in \mathbb{R}^m$ are the state, control input, disturbance, and performance output vectors at time step k, respectively. It will be useful to define the signal $v(k) = \hat{B}w(k)$.

Consider a linear state feedback control law of the form $U(s) = K(s)X(s)$ where K is a dynamic controller. The closed-loop transfer function mapping disturbance w to output y is $T_{w\to y}(s)$, and $T_{w\to u}(s)$, $T_{v\to x}(s)$, and $T_{v\to u}(s)$ are defined analogously. Let $T_{\text{des}}(s)$ be some desired closed-loop transfer function for model matching control design, which can also be set to zero if preferred.

The goal of this paper is to design a controller $K(s)$ that is a solution to the mixed $\mathcal{H}_2/\mathcal{H}_\infty$ control design problem given by

$$\begin{aligned} \underset{K(s)}{\text{minimize}} \quad & \left\| \begin{bmatrix} Q & 0 \\ 0 & R \end{bmatrix} \begin{bmatrix} T_{w\to y}(s) - T_{\text{des}}(s) \\ T_{w\to u}(s) \end{bmatrix} \right\|_{\mathcal{H}_2/\mathcal{H}_\infty} \\ \text{subject to} \quad & T_{v\to x}(s), T_{v\to u}(s) \in \frac{1}{s}\mathcal{RH}_\infty \end{aligned} \tag{2}$$

where the mixed $\mathcal{H}_2/\mathcal{H}_\infty$ norm is given by $\|T\|_{\mathcal{H}_2/\mathcal{H}_\infty} = \|T\|_{\mathcal{H}_2} + \lambda\|T\|_{\mathcal{H}_\infty}$ for some constant $\lambda \in (0,\infty)$. The constant positive semidefinite matrices Q and R represent the weights on output and input, respectively. Note that (2) is nonconvex in $K(s)$ since $T_{w\to y}(s)$ and $T_{w\to u}(s)$ are, so this problem is challenging to solve in this form.

B. System Level Synthesis

Using SLS, (2) can be equivalently reformulated as follows

$$\underset{\Phi_x(s),\Phi_u(s)}{\text{minimize}} \quad \left\| \begin{bmatrix} Q & 0 \\ 0 & R \end{bmatrix} \begin{bmatrix} \tilde{\Phi}_x(s) - T_{\text{des}}(s) \\ \tilde{\Phi}_u(s) \end{bmatrix} \right\|_{\mathcal{H}_2/\mathcal{H}_\infty} \tag{3a}$$

$$\text{subject to} \quad (sI - A)\Phi_x(s) - B\Phi_u(s) = I \tag{3b}$$

$$\Phi_x(s), \Phi_u(s) \in \frac{1}{s}\mathcal{RH}_\infty \tag{3c}$$

where $\Phi_x(s)$ and $\Phi_u(s)$ are the design variables. After solving (3) for $\Phi_x(s)$ and $\Phi_u(s)$, if the controller is selected to be $K(s) = \Phi_u(s)\Phi_x(s)^{-1}$, then the additional affine constraint (3b) ensures that $\Phi_x = T_{v\to x}$, $\Phi_u = T_{v\to u}$, $\tilde{\Phi}_x(s) = C\Phi_x(s)\hat{B}$ and $\tilde{\Phi}_u(s) = \Phi_u(s)\hat{B}$. In other words, the decision variables become the true closed-loop responses due to this SLS constraint. We refer the readers to [2], [5] for further details about SLS. Note that (3c) ensures stability and well-posedness of the closed-loop system. Note that (3) is now convex, although still infinite dimensional as $\Phi_x(s)$ and $\Phi_u(s)$ lie in the infinite dimensional Hardy space $\frac{1}{s}\mathcal{RH}_\infty$, so it is intractable to solve in this form.

IV. Main Results

A. Simple Pole Approximation in Continuous Time

First, we develop a novel finite dimensional approximation to continuous time Hardy space which we call the simple pole approximation (SPA). We show that this can be used to approximate any transfer function in Hardy space, including those with repeated poles, to arbitrary accuracy.

For any $S \in \frac{1}{s}\mathcal{RH}_\infty$, let $\mathcal{Q}$ be the poles of S. For each pole $q \in \mathcal{Q}$, let m_q be its multiplicity in S and let $m_{\max}$ be the maximum multiplicity, i.e., $m_{\max} = \max_{q\in\mathcal{Q}} m_q$. Then the partial fraction decomposition of S can be written

$$S(s) = \sum_{q\in\mathcal{Q}} \sum_{j=1}^{m_q} G_{(q,j)} \frac{1}{(s-q)^j}$$

for some constant coefficient matrices $G_{(q,j)}$. Let $\mathcal{P}$ be a set of simple and distinct poles, hereafter referred to as approximating poles, which will be used to construct a transfer function for approximating S (i.e., $S \approx \sum_{p\in P} G_p \frac{1}{s-p}$). The key idea is that for each pole $q \in \mathcal{Q}$, an approximating transfer function is constructed to approximate q's contribution to the partial fraction decomposition of S. The poles of this approximation are selected to be the m_q closest poles in $\mathcal{P}$ to q, which we denote by $\mathcal{P}(q)$. Then, the overall approximating transfer function for S is obtained by summing over the individual approximating transfer functions for each $q \in \mathcal{Q}$.

We make the following assumptions regarding the set of approximating poles $\mathcal{P}$ and the control design problem.

(A1) *There exists a compact set $\mathcal{K} \subset \mathbb{C}^-$ such that $\mathcal{P}, \mathcal{Q} \subset \mathcal{K}$.*
(A2) $|\mathcal{P}| \geq m_{\max}$.
(A3) *$\mathcal{P}$ is closed under complex conjugation (i.e., $p \in \mathcal{P}$ implies that $\overline{p} \in \mathcal{P}$).*
(A4) *Let $\sigma \subset \mathcal{K}$ be finite. Then for every $q \in \mathcal{Q}$ and every $\lambda \in \sigma$ with $\lambda \neq q, \lambda \notin \mathcal{P}(q)$.*

Assumption A1 ensures that $\mathcal{P}$ and $\mathcal{Q}$ consist of stable poles, and is important for bounding the worst-case approximation error. As $\mathcal{P}$ and $\mathcal{Q}$ are finite, there always exists a compact set $\mathcal{K}$ that contains them. Assumption A2 requires that the size of $\mathcal{P}$ is at least as large as $m_{\max}$. Assumption A3 guarantees that $\mathcal{P}$ can be used to construct a transfer function with real coefficients, and Assumption A4 will be useful once SPA is combined with SLS to maintain a positive distance between plant poles and local approximating poles, and can be easily satisfied in practice.

To bound the approximation error, for each $q \in \mathcal{Q}$ let $\hat{d}(q)$ be the distance from q to the furthest of the m_q simple poles being used to approximate it, i.e., $\hat{d}(q) = \max_{p\in\mathcal{P}(q)} |p-q|$. Let $D(\mathcal{P})$ be the maximum of these distances over all the poles in $\mathcal{Q}$, i.e., $D(\mathcal{P}) = \max_{q\in\mathcal{Q}} \hat{d}(q)$. Then $D(\mathcal{P})$ represents the largest distance between approximating poles in $\mathcal{P}$ and the poles in $\mathcal{Q}$ they are being used to approximate, so it measures the worst-case geometric error in this pole approximation. Intuitively one might therefore expect that as $D(\mathcal{P}) \to 0$, the approximating transfer function would approach S. This intuition is formalized in Theorem 1, which provides an approximation error bound in terms of $\mathcal{H}_2$ and $\mathcal{H}_\infty$ norms of the SPA that is linear in $D(\mathcal{P})$. Thus, Theorem 1 shows that the simple pole approximating transfer function converges to S at least linearly with $D(\mathcal{P})$ and, therefore, that this convergence rate depends purely on the geometry of the pole selection.

Theorem 1 (Simple pole approximation)**.** *Let $S \in \frac{1}{s}\mathcal{RH}_\infty$ and let $\mathcal{P}$ be a set of poles satisfying Assumptions A1-A3. Then there exist constants $c_S = c_S(\mathcal{Q}, G_{(q,j)}, \mathcal{K}) > 0$ and $c'_S = c'_S(\mathcal{Q}, G_{(q,j)}, \mathcal{K}) > 0$, and constant matrices $\{G_p\}_{p\in\mathcal{P}}$ such that $\sum_{p\in\mathcal{P}} G_p \frac{1}{s-p} \in \frac{1}{s}\mathcal{RH}_\infty$ and*

$$\left\| \sum_{p\in\mathcal{P}} G_p \frac{1}{s-p} - S \right\|_{\mathcal{H}_2} \leq c_S D(\mathcal{P}) \tag{4}$$

$$\left\| \sum_{p\in\mathcal{P}} G_p \frac{1}{s-p} - S \right\|_{\mathcal{H}_\infty} \leq c'_S D(\mathcal{P}). \tag{5}$$

Note that the constants c_S and c'_S appearing in Theorem 1 depend on $S \in \frac{1}{s}\mathcal{RH}_\infty$ and on the diameter $\ell(\mathcal{K})$ of the compact set $\mathcal{K}$ in which $\mathcal{P}$ is contained, and do not otherwise depend on the specific pole selection $\mathcal{P}$. This feature will play a crucial role in the following.

Toward that end, we define a sequence of poles, denoted $\{\mathcal{P}_n\}_{n=1}^\infty$, to be a sequence where for each n, $\mathcal{P}_n$ is a finite collection of poles contained in $\mathcal{K}$ and closed under complex conjugation. We say that a sequence of poles $\{\mathcal{P}_n\}_{n=1}^\infty$ is space-filling if it is a sequence of pole selections such that $\mathcal{P}_n \to \mathcal{K}$ with respect to the Hausdorff distance, i.e., the pole sequence converges to the entire compact set. For each n, the space of SPAs from the poles selection $\mathcal{P}_n$ is denoted as $\mathcal{A}_n := \{\sum_{p\in\mathcal{P}_n} G_p \frac{1}{s-p} \in \frac{1}{s}\mathcal{RH}_\infty : G_p \in \mathbb{C}^{\hat{n}\times\hat{m}}\}$.

Theorem 2 (Density in Hardy space)**.** *Let $\{\mathcal{P}_n\}_{n=1}^\infty$ be a space-filling sequence of poles. Then*

$$\lim_{n\to\infty} \mathcal{A}_n = \frac{1}{s}\mathcal{RH}_\infty$$

with respect to both the $\mathcal{H}_2$ and $\mathcal{H}_\infty$ distances.

For any $k > 0$, we say that a sequence of poles $\{\mathcal{P}_n\}_{n=1}^\infty$ has a geometric convergence rate $\frac{1}{n^k}$ if for each $S \in \frac{1}{s}\mathcal{RH}_\infty$ there exists a constant $c_S > 0$ such that $D\left(\mathcal{P}_n\right) \le \frac{c_S}{n^k}$ for all positive integers n. Note that this is in fact a uniform convergence rate since the rate k is independent of the choice of $S \in \frac{1}{s}\mathcal{RH}_\infty$. Theorem 3 shows that if a sequence of poles has geometric convergence rate $\frac{1}{n^k}$, then for any $S \in \frac{1}{s}\mathcal{RH}_\infty$ the simple pole approximation converges to S in the $\mathcal{H}_2$ and $\mathcal{H}_\infty$ norms at the rate $\frac{1}{n^k}$.

Theorem 3 (Uniform convergence rate)**.** *For some $k > 0$, let $\{\mathcal{P}_n\}_{n=1}^\infty$ be a sequence of poles with geometric convergence rate $\frac{1}{n^k}$. Then for any $S \in \frac{1}{s}\mathcal{RH}_\infty$, there exist constants $c_S = c_S(\mathcal{Q}, G_{(q,j)}, \mathcal{K}) > 0$, $c'_S = c'_S(\mathcal{Q}, G_{(q,j)}, \mathcal{K}) > 0$, and $N > 0$ such that for any $n \ge N$ there exist $\{G_p^n\}_{p\in\mathcal{P}_n}$ such that $\sum_{p\in\mathcal{P}_n} G_p^n \frac{1}{s-p} \in \frac{1}{s}\mathcal{RH}_\infty$ and*

$$\left\| \sum_{p\in\mathcal{P}_n} G_p^n \frac{1}{s-p} - S \right\|_{\mathcal{H}_2} \le \frac{c_S}{n^k} \tag{6}$$

$$\left\| \sum_{p\in\mathcal{P}_n} G_p^n \frac{1}{s-p} - S \right\|_{\mathcal{H}_\infty} \le \frac{c'_S}{n^k}. \tag{7}$$

As we are attempting to approximate a transfer function S whose poles are not in general known in advance, a natural choice for poles in the selection for SPA would be to choose them uniformly (i.e., evenly spaced) over $\mathcal{K}$ in order to maximize the probability that every pole in S has a nearby approximating pole in the SPA selection. However, since finding exactly uniformly spaced pole selections over $\mathcal{K}$ is a challenging problem in general - typically nonconvex - and since analytic expressions for the approximating poles help facilitate the derivation of meaningful error bounds, we resort to finding approximately uniform pole selections instead. As a special case of practical interest, the compact set $\mathcal{K} \subset \mathbb{C}^-$ in Assumption A1 is selected to be a trapezoidal region, which is a practical approximation of the stable region in the continuous time complex plane, commonly used in model reduction and control design to restrict pole locations to a bounded subset of the open left half plane (see e.g., [15], [16]). A commonly used heuristic for generating approximately evenly spaced points over arbitrary shapes is to select the centers of uniformly spaced grid cells, a method that has proven effective in various applications including numerical analysis and control design (e.g., [17]). Let $\bar{l}$ be the minimum between half the height and half the shorter base of the trapezoid $\mathcal{K}$. We adopt this approach by overlaying a grid of uniform cells of length l on the trapezoid, where $l \le \bar{l}$, and selecting the approximating poles $\mathcal{P}$ to be the centers of all such cells that are entirely contained in the trapezoid, as shown in Fig. 1. Let θ denote the trapezoidal base angle as shown in Fig. 1. Let $n(l)$ denote the number of selected poles under grid size l, and let $P_{n(l)}$ be the resulting set of poles. Note that $n(l) \to \infty$ as $l \to 0$. Theorem 4 provides a geometric convergence rate for this trapezoid pole selection.

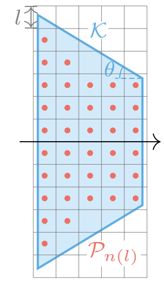

Fig. 1. The trapezoidal region $\mathcal{K}$ in the open left half plane overlaid with a uniform grid and the pole selection from the centers of grid cells.

Theorem 4 (Trapezoid geometric convergence rate)**.** *Let $\mathcal{K} \subset \mathbb{C}^-$ and $\mathcal{P}_{n(l)}$ be the trapezoid and the trapezoid pole selection as defined above. Define the set of achievable poles $\mathcal{N} := \{n \in \mathbb{Z}^+ : \exists 0 < l \le \bar{l},\ \mathcal{P}_n = \mathcal{P}_{n(l)}\}$ Then, for each $n \in \mathcal{N}$,*

$$D(\mathcal{P}_n) \le \frac{c_S}{n^{1/2}}, \tag{8}$$

$$c_S = (m_{\max} - 1)\,\bar{l} + d_{\max}, \tag{9}$$

$$d_{\max} = \bar{l}\sqrt{13/4 + \lceil \tan\theta \rceil^2 + 3\lceil \tan\theta \rceil}. \tag{10}$$

Corollary 1 shows that for for this trapezoid pole selection, the SPA converges to the full Hardy space at a rate of $n^{1/2}$ in the $\mathcal{H}_2$ and $\mathcal{H}_\infty$ norms.

Corollary 1 (Trapezoid approximation convergence rate)**.** *Consider the pole selection of Theorem 4. Then for any $S \in \frac{1}{s}\mathcal{RH}_\infty$ there exist constants $c_S = c_S(\mathcal{Q}, G_{(q,j)}, \mathcal{K}) > 0$, $c'_S = c'_S(\mathcal{Q}, G_{(q,j)}, \mathcal{K}) > 0$, and $N > 0$ such that for each integer $n \in \mathcal{N}$ with $n \ge N$, there exist $\{G_p^n\}_{p\in\mathcal{P}_n}$ such that*

$$\left\| \sum_{p\in\mathcal{P}_n} G_p^n \frac{1}{s-p} - S \right\|_{\mathcal{H}_2} \le \frac{c_S}{n^{1/2}} \tag{11}$$

$$\left\| \sum_{p\in\mathcal{P}_n} G_p^n \frac{1}{s-p} - S \right\|_{\mathcal{H}_\infty} \le \frac{c'_S}{n^{1/2}}. \tag{12}$$

B. Mixed $\mathcal{H}_2/\mathcal{H}_\infty$ Control with System Level Synthesis in Continuous Time

In this subsection we develop the first tractable and convex method for $\mathcal{H}_2/\mathcal{H}_\infty$ control design in continuous time with SLS. The following Assumption A5 is a standard feasibility assumption, and we adopt it for the remainder of the paper.

(A5) A solution to (2) exists, i.e., (A, B) is stabilizable, and the optimal closed-loop transfer functions are rational (hence they have finitely many poles).

SPA developed in Subsection IV-A is a potential approach to addressing the infinite dimensionality of (3). To do so, we first specify a pole selection $\mathcal{P}$ for SPA. In particular, we choose $\mathcal{P}$ to consist of the plant poles (to guarantee feasibility), any optimal poles known a priori (to reduce suboptimality), and the remaining poles obtained via the trapezoid pole selection in Subsection IV-A, which ensures that the approximating poles converge to each optimal pole.

Using SPA for the closed-loop transfer functions Φ_x and Φ_u from (3) results in

$$\Phi_x(s) = \sum_{p\in\mathcal{P}} G_p \frac{1}{s-p} \qquad \Phi_u(s) = \sum_{p\in\mathcal{P}} H_p \frac{1}{s-p}, \tag{13}$$

where $G_p \in \mathbb{C}^{n\times n}$ and $H_p \in \mathbb{C}^{p\times n}$ are coefficient matrices for each $p \in \mathcal{P}$, which renders (3) finite dimensional but still requires a method for efficient evaluation of the $\mathcal{H}_2/\mathcal{H}_\infty$ norms. A state space realization $(\tilde{A}, \tilde{B}, \tilde{C}, 0)$ for the closed-loop transfer function appearing in the objective function (3a) is developed, and then the $\mathcal{H}_2$ and $\mathcal{H}_\infty$ norms are reexpressed as LMIs by the KYP lemma using this closed-loop realization. The state space realizations are carefully designed so that this construction results in LMIs; alternative choices would lead to BMIs, which are nonconvex. Moreover, since the additional constraint required by SLS in (3b) would become nonconvex under a state space reformulation, instead it is retained in the frequency domain to ensure that it remains affine.

Combining these two representations, we obtain the following control design formulation for the solution to (3) with the SPA (13)

$$\underset{K_1, K_2, Z, G_p, H_p, \gamma_1, \gamma_2}{\text{minimize}} \quad \gamma_1 + \lambda\gamma_2 \tag{14a}$$

$$\text{subject to} \quad \begin{bmatrix} -\tilde{A}^\intercal K_1 - K_1\tilde{A}^\intercal & -K_1\tilde{B} \\ -\tilde{B}^\intercal K_1 & \gamma_1 I \end{bmatrix} \succ 0 \tag{14b}$$

$$\begin{bmatrix} K_1 & \tilde{C}(G_p, H_p)^\intercal \\ \tilde{C}(G_p, H_p) & Z \end{bmatrix} \succ 0 \tag{14c}$$

$$\mathrm{Tr}(Z) < \gamma_1 \tag{14d}$$

$$\begin{bmatrix} -\tilde{A}^\intercal K_2 - K_2\tilde{A} & -K_2\tilde{B} & -\tilde{C}(G_p, H_p)^\intercal \\ -\tilde{B}^\intercal K_2 & \gamma_2 I & 0 \\ -\tilde{C}(G_p, H_p) & 0 & \gamma_2 I \end{bmatrix} \succ 0 \tag{14e}$$

$$\sum_{p\in\mathcal{P}} G_p = I \tag{14f}$$

$$\forall p \in \mathcal{P}, \qquad (pI - A)G_p - BH_p = 0 \tag{14g}$$

where $K_1, K_2 \in \mathbb{S}^{n|\mathcal{P}|}$, $Z \in \mathbb{S}^m$, and γ_1, γ_2 are scalar variables that represent the $\mathcal{H}_2$ and $\mathcal{H}_\infty$ norms of the closed-loop transfer functions, respectively. Note that for a fixed collection of simple poles $\mathcal{P}$, as used for SPA, $\tilde{A}$ and $\tilde{B}$ are constant matrices, and $\tilde{C}$ is an affine function of all of the variable coefficients G_p and H_p for all $p \in \mathcal{P}$. Further details will be provided in Section V.

Thus, the objective (14a) is linear, the constraints (14b)-(14e) are LMIs in the decision variables, and both of them are derived from a state space representation. The SLS constraints (14g) and (14f) are linear and affine respectively in the frequency domain. Therefore, overall the control design optimization problem (14) is a convex SDP that can be solved efficiently.

Our main theoretical result for this Subsection shows that the relative error of the proposed control design method decays at least linearly with $D(\mathcal{P})$. Here, $G^*_{(q,j)}$ and $H^*_{(q,j)}$ denote the coefficients in the partial fraction decomposition of an optimal solution to (3), and σ denotes the set of stable plant poles.

Theorem 5 (General suboptimality bound)**.** *Let J^* denote the optimal cost of the infinite dimensional problem (2), and let $J(\mathcal{P})$ denote the optimal cost of (14) as a function of the pole selection $\mathcal{P}$. Suppose $\mathcal{P}$ satisfies Assumptions A1-A4. Then there exists a constant $\hat{K} = \hat{K}(\mathcal{Q}, G^*_{(q,j)}, H^*_{(q,j)}, \mathcal{K}, \sigma) > 0$ such that*

$$\frac{J(\mathcal{P}) - J^*}{J^*} \le \hat{K} D(\mathcal{P}). \tag{15}$$

Corollary 2 shows that, for the trapezoid pole selection in Theorem 4, the relative error of SPA converges to zero at a rate of $n^{1/2}$. This ensures that the solution to (14) will converge to the ground-truth infinite dimensional solution to (2) as the number of approximating poles approaches infinity. Furthermore, it provides a specific worst-case uniform convergence rate for this suboptimality bound based purely on the geometry of the trapezoid pole selection.

Corollary 2 (Trapezoid suboptimality bound)**.** *Consider the setting of Theorem 5 with pole selection $\mathcal{P}_n$ given as in Theorem 4 for each integer $n \in \mathcal{N}$. Then there exists a constant $\hat{K} = \hat{K}(\mathcal{Q}, G^*_{(q,j)}, H^*_{(q,j)}, \mathcal{K}, \sigma) > 0$ and $N > 0$ such that for each integer $n \in \mathcal{N}$ with $n \ge N$*

$$\frac{J(\mathcal{P}) - J^*}{J^*} \le \frac{\hat{K}}{n^{1/2}}. \tag{16}$$

Notably, the design method (14) exactly determines the $\mathcal{H}_2$ and $\mathcal{H}_\infty$ norms of the closed-loop transfer function, and so does not require any further approximations to compute these norms. As a result, for the trapezoid pole selection proposed in Theorem 4, the suboptimality bound (16) applies exactly to (14), and ensures that the suboptimality converges to zero as the number of poles approaches infinity. As we will see in the numerical example in Section VI, even a small number of poles can often result in low suboptimality, and thus good performance, in practice.

V. Control Design Derivation

The goal of this section is to develop a control design method for solving (3), the SLS reformulation of the mixed $\mathcal{H}_2/\mathcal{H}_\infty$ control design problem in continuous time. Towards that end, we first reexpress the SLS constraint (3b) using

SPA and construct a state space realization of the closed-loop transfer functions. Then, we will see that the $\mathcal{H}_2$ and $\mathcal{H}_\infty$ norms in the objective (3a) can be evaluated using the continuous time KYP lemma. Finally, combining this KYP reformulation with the SLS constraint in (3b) and SPA will yield the desired control design method.

After substituting the SPA (13) into the SLS constraint (3b) and matching coefficients of $\frac{1}{s-p}$ for each pole $p \in \mathcal{P}$ since these functions are linearly independent, we obtain

$$\sum_{p\in\mathcal{P}} G_p = I^n \tag{17}$$

$$(pI^n - A)\, G_p - BH_p = 0^n, \qquad \forall p \in \mathcal{P}. \tag{18}$$

Since $\Phi_x(s)$ and $\Phi_u(s)$ are real, it is straightforward to show that for any real pole p, G_p and H_p are real, and for any complex pole p, $G_{\overline{p}} = \overline{G_p}$ and $H_{\overline{p}} = \overline{H_p}$. Let $\mathcal{P}_r$ denote the real poles in $\mathcal{P}$, and let $\mathcal{P}_c$ denote its complex poles. Then $\mathcal{P} = \mathcal{P}_r \cup \mathcal{P}_c$. For any $p \in \mathcal{P}_c$, its conjugate $\overline{p}$ is also in $\mathcal{P}_c$, and their corresponding coefficient matrices are:

$$\begin{aligned} G_p &= \mathrm{Re}(G_p) + \mathrm{Im}(G_p)j \quad & G_{\overline{p}} &= \mathrm{Re}(G_p) - \mathrm{Im}(G_p)j \\ H_p &= \mathrm{Re}(H_p) + \mathrm{Im}(H_p)j \quad & H_{\overline{p}} &= \mathrm{Re}(H_p) - \mathrm{Im}(H_p)j. \end{aligned} \tag{19}$$

This is a finite dimensional and affine reexpression of the SLS constraint (3b) using SPA.

Next to derive the proposed control design method, we will require state space realizations of the closed-loop transfer functions. We first find real state space realizations for $\tilde{\Phi}_x(s)$ and $\tilde{\Phi}_u(s)$. To do so, for each complex conjugate pair $p, \overline{p} \in \mathcal{P}_c$, define the matrix

$$\hat{M}_p = \begin{bmatrix} \mathrm{Re}(p) & \mathrm{Im}(p) \\ -\mathrm{Im}(p) & \mathrm{Re}(p) \end{bmatrix},$$

and let $\mathcal{M}_c$ be the collection of $\hat{M}_p$ for all such complex conjugate pairs. Let $\mathcal{M}_r$ be the collection of each scalar p for all $p \in \mathcal{P}_r$. Then we can define

$$\overline{A} = \begin{bmatrix} \mathcal{D}(\mathcal{M}_r) & \\ & \mathcal{D}(\mathcal{M}_c) \end{bmatrix} \otimes I^n$$
$$\overline{B} = \big[\underbrace{I^n \ \ \cdots \ \ I^n}_{|\mathcal{P}_r|} \ \ \underbrace{2I^n \ \ 0^n \ \ \cdots \ \ 2I^n \ \ 0^n}_{|\mathcal{P}_c|}\big]^\intercal \hat{B}.$$

Next, for each complex conjugate pair $p, \overline{p} \in \mathcal{P}_c$, define the matrices

$$\hat{G}_p = \begin{bmatrix} \mathrm{Re}(G_p) & \mathrm{Im}(G_p) \end{bmatrix} \quad \hat{H}_p = \begin{bmatrix} \mathrm{Re}(H_p) & \mathrm{Im}(H_p) \end{bmatrix},$$

and let $\mathcal{G}_c$ and $\mathcal{H}_c$ be the collection of $\hat{G}_p$ and $\hat{H}_p$, respectively, for all such complex conjugate pairs. Let $\mathcal{G}_r$ and $\mathcal{H}_r$ be the collection of G_p and H_p, respectively, for each $p \in \mathcal{P}_r$. Then we define

$$\overline{C}_x = C \begin{bmatrix} \mathcal{R}(\mathcal{G}_r) & \mathcal{R}(\mathcal{G}_c) \end{bmatrix} \quad \overline{C}_u = \begin{bmatrix} \mathcal{R}(\mathcal{H}_r) & \mathcal{R}(\mathcal{H}_c) \end{bmatrix}.$$

It is straightforward to verify that $(\overline{A}, \overline{B}, \overline{C}_x, 0)$ is a real state space realization of $\tilde{\Phi}_x(s)$, and that $(\overline{A}, \overline{B}, \overline{C}_u, 0)$ is a real state space realization of $\tilde{\Phi}_u(s)$. To see this, first note that since $\overline{A}$ is block diagonal, $\overline{C}_x(sI - \overline{A})^{-1}\overline{B}$ and $\overline{C}_u(sI - \overline{A})^{-1}\overline{B}$ can be decomposed into the contributions from individual real poles and from complex conjugate pairs of poles. For any real pole p, it follows

$$CG_p \left[sI - pI\right]^{-1} \hat{B} = CG_p \frac{1}{s-p} \hat{B}.$$

For any complex conjugate pair of poles p and $\overline{p}$,

$$\begin{aligned} &\begin{bmatrix} \mathrm{Re}(G_p) & \mathrm{Im}(G_p) \end{bmatrix} \begin{bmatrix} sI - \mathrm{Re}(p)I & -\mathrm{Im}(p)I \\ \mathrm{Im}(p)I & sI - \mathrm{Re}(p)I \end{bmatrix}^{-1} \begin{bmatrix} 2I \\ 0 \end{bmatrix} \\ &= \begin{bmatrix} \mathrm{Re}(G_p) & \mathrm{Im}(G_p) \end{bmatrix} \frac{1}{(s-p)(s-\overline{p})} \begin{bmatrix} 2sI - 2\mathrm{Re}(p)I \\ -2\mathrm{Im}(p)I \end{bmatrix} \\ &= \frac{2s\mathrm{Re}(G_p) - 2\mathrm{Re}(G_p)\mathrm{Re}(p) - 2\mathrm{Im}(G_p)\mathrm{Im}(p)}{(s-p)(s-\overline{p})} \\ &\overset{(19)}{=} G_p \frac{1}{s-p} + G_{\overline{p}} \frac{1}{s-\overline{p}}. \end{aligned} \tag{20}$$

Thus, overall (combining (20) and (13) over all poles in $\mathcal{P}$) we obtain $C_x(sI - A)^{-1}B = C(\sum G_p \frac{1}{s-p})\hat{B} = C\Phi_x B = \tilde{\Phi}_x$. Therefore, $(\overline{A}, \overline{B}, \overline{C}_x, 0)$ is a real state space realization of $\tilde{\Phi}_x(s)$, and $(\overline{A}, \overline{B}, \overline{C}_u, 0)$ can be shown to be a real state space realization of $\tilde{\Phi}_u(s)$ analogously.

Let $(A_{\text{des}}, B_{\text{des}}, C_{\text{des}}, 0)$ be any real state space realization of T_{des}. Now we can represent the transfer function in the objective (3a) using the following real state space realization

$$\tilde{A} = \begin{bmatrix} \overline{A} & 0 \\ 0 & A_{\text{des}} \end{bmatrix} \quad \tilde{B} = \begin{bmatrix} \overline{B} \\ B_{\text{des}} \end{bmatrix} \quad \tilde{C} = \begin{bmatrix} Q\overline{C}_x & -QC_{\text{des}} \\ R\overline{C}_u & 0 \end{bmatrix}, \tag{21}$$

which satisfies

$$\tilde{C}(sI - \tilde{A})^{-1}\tilde{B} = \begin{bmatrix} Q & 0 \\ 0 & R \end{bmatrix} \begin{bmatrix} \tilde{\Phi}_x(s) - T_{\text{des}}(s) \\ \tilde{\Phi}_u(s) \end{bmatrix} =: \tilde{\Phi}(s). \tag{22}$$

Thus, we have obtained an equivalent state space representation of the closed-loop transfer function $\tilde{\Phi}(s)$. Note that we have carefully constructed the state space realizations such that for a fixed collection of simple poles $\mathcal{P}$, as used for SPA, $\tilde{A}$ and $\tilde{B}$ are constant matrices, and $\tilde{C}$ is an affine function of all of the variable coefficients G_p and H_p.

The objective (3a) is to minimize $\|\tilde{\Phi}\|_{\mathcal{H}_2} + \lambda\|\tilde{\Phi}\|_{\mathcal{H}_\infty}$. This can be expressed as an equivalent optimization problem

$$\underset{\gamma_1,\gamma_2}{\text{minimize}} \qquad \gamma_1 + \lambda\gamma_2 \tag{23a}$$
$$\text{subject to} \quad \|\tilde{\Phi}(z)\|_{\mathcal{H}_2} < \gamma_1 \tag{23b}$$
$$\|\Phi(z)\|_{\mathcal{H}_\infty} < \gamma_2 \tag{23c}$$

because these two inequalities will become tight at optimality. Since $\tilde{A}$ consists of all stable poles in $\mathcal{P}$, $\tilde{A}$ is naturally Hurwitz, and we apply the KYP lemma to reexpress the constraints bounding the $\mathcal{H}_2$ and $\mathcal{H}_\infty$ norms using our state space representation $(\tilde{A}, \tilde{B}, \tilde{C}, 0)$. We require the following form of the KYP lemma:

KYP lemma [18, Section 3.3]: For the transfer function $\tilde{\Phi}(s) = \tilde{C}(sI - \tilde{A})^{-1}\tilde{B}$, if $\tilde{A}$ is Hurwitz then the following statements hold.

1) $\|\tilde{\Phi}(s)\|_{\mathcal{H}_2} < \gamma_1$ if and only if there exist $K_1 \in \mathbb{S}^{n|\mathcal{P}|}$, $Z \in \mathbb{S}^m$, such that

$$\begin{bmatrix} \tilde{A}^\intercal K_1 + K_1\tilde{A} & K_1\tilde{B} \\ \tilde{B}^\intercal K_1 & -\gamma_1 I \end{bmatrix} \prec 0 \quad \begin{bmatrix} K_1 & \tilde{C}^\intercal \\ \tilde{C} & Z \end{bmatrix} \succ 0 \quad \mathrm{Tr}(Z) < \gamma_1. \tag{24}$$

2) $\|\tilde{\Phi}(s)\|_{\mathcal{H}_\infty} < \gamma_2$ if and only if there exists $K_2 \in \mathbb{S}^{n|\mathcal{P}|}$,

$$\begin{bmatrix} \tilde{A}^\intercal K_2 + K_2\tilde{A} & K_2\tilde{B} & \tilde{C}^\intercal \\ \tilde{B}^\intercal K_2 & -\gamma_2 I & 0 \\ \tilde{C} & 0 & -\gamma_2 I \end{bmatrix} \prec 0. \tag{25}$$

Now we can apply the KYP lemma to reexpress the constraints (23b) and (23c) as (24) and (25). Note that for a fixed set of poles $\mathcal{P}$, as is used for SPA, since $\tilde{A}$ and $\tilde{B}$ are constant matrices and $\tilde{C}$ is affine in the decision variables, (24) and (25) are LMIs. Hence, the careful construction of the state space realizations in this section avoided the potential nonconvex BMIs that could have occurred. Combining these LMI constraints (24)-(25) with the objective (23a) and the SLS constraints (17)-(18) results in the final control design formulation as shown in (14).

VI. Numerical Example

In this section, we demonstrate the proposed control synthesis method on the control of a wind turbine interfaced to the power grid via a power converter. We model the turbine and converter system using the model proposed in [13]. Let w be a vector whose components represent the frequency and voltage magnitude of the AC voltage at the connection point, respectively, and let y represent the active and reactive power output of the converter. To improve grid performance, our goal is to design fast frequency and voltage control and to enforce decoupling between their respective control loops. To do so, we choose a desired closed-loop transfer function that we attempt to match in design, which is diagonal and whose diagonal elements are low pass filters with equal time constants. This represents a challenging scenario for the control design because the two control loops operate on the same time scale, so they cannot be decoupled via timescale separation. Then this can be formulated in the form of (1) with matrices given by

$$A = \begin{bmatrix} -11.725 & 0 & 0 & 0 & 0 \\ 0 & -60 & 7.0606 & -0.6729 & -7.9931 \\ 60 & 0 & -60 & 0 & 0 \\ 0 & 0 & 0 & -0.6667 & 0 \\ 0 & 0 & 0 & 0 & -60 \end{bmatrix} \quad B = \begin{bmatrix} 0 & 0 \\ 0 & 0 \\ 0 & 0 \\ 0.6667 & 0 \\ 0 & 60 \end{bmatrix}$$

$$C = \begin{bmatrix} 0 & 0.9066 & -0.0364 & 1.0218 & 0 \\ 0 & 0.0364 & 0.9066 & -0.2406 & -1.0201 \end{bmatrix} \quad \hat{B} = \begin{bmatrix} -29.3125 & 0 \\ 0 & 60.414 \\ 150 & 0 \\ 0 & 0 \\ 0 & 0 \end{bmatrix}$$

$$A_{\mathrm{des}} = \begin{bmatrix} -1.4286 & \\ & -1.4286 \end{bmatrix} \quad B_{\mathrm{des}} = \begin{bmatrix} -28.4275 & \\ & -29.2857 \end{bmatrix} \quad C_{\mathrm{des}} = I_2.$$

where $(A_{\mathrm{des}}, B_{\mathrm{des}}, C_{\mathrm{des}}, 0)$ is a state space realization of the desired transfer function, as discussed in Section V.

For the control design, we choose $Q = I_2$, $R = 0.01 I_2$, and $\lambda = 0.5$. For the SPA pole selection $\mathcal{P}$, we first incorporate the plant poles and the poles of the desired transfer function, and the remaining poles are chosen from the trapezoid pole selection method discussed in Subsection IV-A with a grid length $l = 35$ over a trapezoid whose left and right bases are located at -62.8 and -1.3, respectively, and with angle $\theta = \pi/4$. In total, 7 closed-loop poles are selected in $\mathcal{P}$. We solve the SDP (14) for the proposed control design method using MOSEK [19] in conjunction with YALMIP [20] in MATLAB, and obtain the solution within 0.88 seconds.

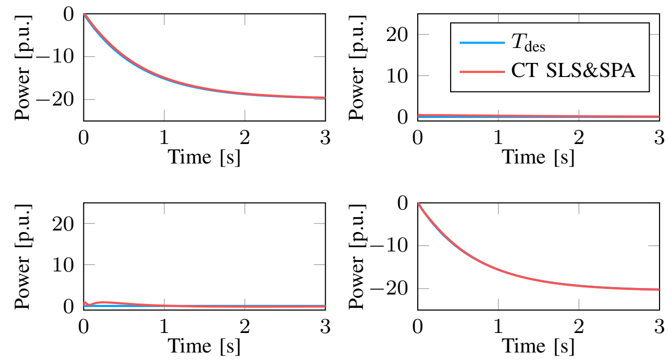

Fig. 2. Step responses of the desired transfer function (T_{des}) and of the solutions of the proposed control design method (CT SLS&SPA).

The MIMO step responses for the desired transfer function and the actual closed-loop transfer functions using the proposed control design method are shown in Fig. 2, which shows almost perfect matching with the desired response. Thus, SLS with SPA in continuous time was successfully used to control a power converter for providing desired frequency and voltage regulation in the power grid.

VII. Proofs

A. *Proofs of Theorems 1, 2 and 3*

The following lemmas present useful identities for developing SPA approximation error bounds for a transfer function with a single repeated pole in the SISO case.

Denote the diameter of $\mathcal{K}$ as $\ell(\mathcal{K}) = \sup_{x,y\in\mathcal{K}} \|x - y\|$.

Lemma 1. *For any positive integer m, let $p_1, \dots, p_m, q \in \mathcal{K}$, $I_m = \{1, 2, \dots, m\}$, and $\mathcal{P} = \cup_{i=1}^m p_i$. Let $\hat{d}(q) = \max_i |p_i - q|$. Let $s = j\omega$, for some $\omega \in \mathbb{R}$. Then there exist constants $c_1, \dots, c_m$ such that*

$$\begin{aligned} &\left| \sum_{i=1}^m c_i \frac{1}{s - p_i} - \frac{1}{(s-q)^m} \right|_{s=j\omega} \\ &\le \frac{((|q|+2)^m - (|q|+1)^m)\ell(\mathcal{K})^{m-1}\hat{d}(q) \sum_{k=0}^{m-1} |\omega|^k}{|j\omega - q|^m \prod_{i=1}^m |j\omega - p_i|} \\ &= \underbrace{\frac{1}{\prod_{i=1}^m |j\omega - p_i|}}_{f(\omega)} \underbrace{\frac{\sum_{k=0}^{m-1} |\omega|^k}{|j\omega - q|^m}}_{g(\omega)} \\ &\quad \cdot ((|q|+2)^m - (|q|+1)^m)\ell(\mathcal{K})^{m-1}\hat{d}(q). \end{aligned} \tag{26}$$

Proof of Lemma 1: Since all poles lie within a compact set $\mathcal{K}$, the approximating distance $\hat{d}(q)$ is finite and bounded by the diameter of $\mathcal{K}$. We have

$$\hat{d}(q)^k = \hat{d}(q)^{k-1}\hat{d}(q) \le \ell(\mathcal{K})^{m-1}\hat{d}(q) \tag{27}$$

for all $k \in I_m$. By [11, Proof of Lemma 3], if we select constants c_i by

$$c_i = \left(\prod_{\substack{j=1 \\ j\neq i}}^m (p_i - p_j) \right)^{-1}, \tag{28}$$

then

$$\sum_{i=1}^{m} c_i \frac{1}{s-p_i} = \left(\prod_{i=1}^{m}(s-p_i)\right)^{-1} \tag{29}$$

for all $i \in I_m$. After choosing constants $\{c_i\}_{i=1}^m$ by (28), to prove the claim, it suffices to show that $\left|\frac{1}{\prod_{i=1}^m (s-p_i)} - \frac{1}{(s-q)^m}\right|$ satisfies (26). We compute

$$\frac{1}{\prod_{i=1}^m (s-p_i)} - \frac{1}{(s-q)^m} = \frac{(s-q)^m - \prod_{i=1}^m (s-p_i)}{(s-q)^m \prod_{i=1}^m (s-p_i)}. \tag{30}$$

Set $s = jw$ for the numerator of the right side of (30)

$$\begin{aligned}
&\left|(s-q)^m - \prod_{i=1}^m (s-p_i)\right| \\
&\overset{\text{[11, Proof of Corollary 2]}}{\leq} \sum_{k=1}^{m} |\omega|^{m-k} \binom{m}{k} ((|q|+\hat{d}(q))^k - |q|^k) \qquad (31)\\
&\overset{\text{adding more terms}}{\leq} \sum_{k=0}^{m-1} |\omega|^k \sum_{k'=1}^{m} \binom{m}{k'} ((|q|+\hat{d}(q))^{k'} - |q|^{k'}) \\
&\overset{\text{[11, Proof of Corollary 2]}}{\leq} \sum_{k=0}^{m-1} |\omega|^k \sum_{k'=1}^{m} \binom{m}{k'} (|q|+1)^{m-k'} \hat{d}(q)^{k'} \\
&\overset{\text{(27), binomial theorem}}{\leq} ((|q|+2)^m - (|q|+1)^m)\ell(\mathcal{K})^{m-1}\hat{d}(q) \sum_{k=0}^{m-1} |\omega|^k. \qquad (32)
\end{aligned}$$

Furthermore, substituting $s = j\omega$ into the denominator of (30) implies that its absolute value is equal to $|j\omega - q|^m \prod_{i=1}^m |j\omega - p_i|$. Thus, we obtain

$$\begin{aligned}
&\left|\frac{1}{\prod_{i=1}^m (s-p_i)} - \frac{1}{(s-q)^m}\right| \\
&\overset{(32)}{\leq} \frac{((|q|+2)^m - (|q|+1)^m)\ell(\mathcal{K})^{m-1}\hat{d}(q)\sum_{k=0}^{m-1}|\omega|^k}{|j\omega - q|^m \prod_{i=1}^m |j\omega - p_i|}.
\end{aligned}$$

□

In the proof of Lemma 1, ω can lie anywhere on the imaginary axis, so its norm is unbounded, and therefore the obtained bounds must be a function of ω. In contrast, in the discrete time setting [11, Corollary 2] the corresponding variable z lies on the unit circle, so its norm is equal to one, and therefore uniform bounds that are independent of z can be easily obtained.

To bound the $\mathcal{H}_2$ and $\mathcal{H}_\infty$ norms between a transfer function with repeated poles and the SPA, we will require Lemmas 2-5. Lemma 2 lower bounds the denominators of $f(\omega)$ and $g(\omega)$ in (26) by an even function, facilitating the simplification of integral computations involved in the $\mathcal{H}_2$ expressions required. Lemma 3 and Lemma 4 present closed-form integral expressions useful for evaluating this $\mathcal{H}_2$ norm. Lemmas 5 provides an expression for the numerator of (26) raised to a power for use in computing this $\mathcal{H}_2$ norm.

Lemma 2 (Lower bounds for denominators)**.** *For any positive integer m, let $p_1, \ldots, p_m \in \mathbb{C}^-$ and $\omega \in \mathbb{R}$. There exist constants a and b such that*

$$\prod_{i=1}^m |j\omega - p_i| \geq (a\omega^2 + b)^{m/2}. \tag{33}$$

Proof of Lemma 2: We first prove there exist a_i', b_i' (with the appropriate bounds) such that $|j\omega - p_i|^2 \geq a_i'\omega^2 + b_i'$ for all $i \in I_m$, and (33) follows immediately.

We compute $|j\omega - p_i|^2 = (\omega - p_i^y)^2 + (p_i^x)^2$, If $p_i^y = 0$ then the desired bound follows trivially by choosing $a_i' = 1$ and $b_i' = (p_i^x)^2$. So, suppose $p_i^y \neq 0$.

Define $m(\omega) = (\omega - p_i^y)^2 + (p_i^x)^2$ and $n(\omega) = a_i'\omega^2 + b_i'$, where a_i' and b_i' are coefficients. To prove the first claim, it suffices to find a_i' and b_i' such that $m(\omega) \geq n(\omega)$ for all $\omega \in \mathbb{R}$. To do so, one intuitive idea is to enforce that $m(\omega)$ and $n(\omega)$ intersect only at a single point (to get a tighter bound) and have the same tangents at that point (so that n is a lower bound of m). Assume ω^* is the intersection point of $m(\omega)$ and $n(\omega)$, it satisfies

$$\begin{aligned}
(\omega^* - p_i^y)^2 + (p_i^x)^2 &= a_i'(\omega^*)^2 + b_i' \qquad \text{(intersection point)}\\
\omega^* - p_i^y &= a_i'\omega^* \qquad \text{(tangent equation).}
\end{aligned}$$

Substituting the tangent equation into the first equation and eliminating ω^* yields

$$a_i' = \frac{(p_i^x)^2 - b_i'}{(p_i^x)^2 + (p_i^y)^2 - b_i'}. \tag{34}$$

Choose $b_i' = (p_i^x)^2/4$, which is an arbitrary choice. Then $a_i' = \frac{3(p_i^x)^2}{3(p_i^x)^2 + 4(p_i^y)^2}$, $\omega^* = \frac{3(p_i^x)^2 + 4(p_i^y)^2}{4p_i^y}$.

Note that $m(\omega) - n(\omega) = (1-a_i')\omega^2 - 2p_i^y\omega + (p_i^y)^2 + (p_i^x)^2 - b_i' \overset{(34)}{=} \frac{(p_i^y)^2}{(p_i^x)^2 + (p_i^y)^2 - b_i'}\left(\omega - \frac{(p_i^x)^2 + (p_i^y)^2 - b_i'}{p_i^y}\right)^2 \geq 0$, which implies that $m(\omega) \geq n(\omega)$ for all $\omega \in \mathbb{R}$. This proves the initial claim.

By the initial claim, after taking the square root there, let $a = \min\{a_i'\}_{i=1}^m$ and $b = \min\{b_i'\}_{i=1}^m$. Then $\prod_{i=1}^m |j\omega - p_i| \geq \prod_{i=1}^m (a_i'\omega^2 + b_i')^{1/2} \geq (a\omega^2 + b)^{m/2}$. □

Lemma 2 provides even functional lower bounds for denominators of $f(\omega), g(\omega)$, which will be meaningful for their integrals with respect to ω.

Lemma 3 (Integral formulas)**.** *Let a, b be any positive real numbers, m be any positive integer, $n \in \{0, \ldots, 2m-1\}$. Then $I_{(m,n)}^{(a,b)} = \int_0^\infty \frac{\omega^n}{(a\omega^2+b)^m} \mathrm{d}\omega$ can be computed via the following formulas:*

$$I_{(m,n)}^{(a,b)} = \left(\frac{\pi}{2}\right)^{\mathcal{I}(n)} \frac{(n-1)!!(2m-n-3)!!}{(2m-2)!! b^{\frac{2m-n-1}{2}} a^{\frac{n+1}{2}}} \tag{35}$$

where the indicator function $\mathcal{I}(n)$ is defined to be 1 when n is even and 0 otherwise.

Proof of Lemma 3: The main idea of the proof is to use induction on the two variables m, n. Ignoring the superscript (a,b) is admissible if there is no ambiguity.

For the base cases, we first prove it for $n = 0$ and $n = 1$:

$$I_{(m,0)} = \int_0^\infty \frac{1}{(a\omega^2+b)^m} \mathrm{d}\omega = \frac{\pi}{2} \frac{(2m-3)!!}{(2m-2)!! b^{\frac{2m-1}{2}} a^{\frac{1}{2}}}$$

$$I_{(m,1)}=\int_0^\infty \frac{\omega}{(a\omega^2+b)^m}\,\mathrm{d}\omega=\frac{1}{2(m-1)b^{m-1}a}$$

for all $m\geq 1$. To do so, we first show it for the base case $(1,0)$:

$$I_{(1,0)}=\int_0^\infty \frac{1}{a\omega^2+b}\,\mathrm{d}\omega \overset{u=\frac{\sqrt{a}\omega}{\sqrt{b}}}{=} \int_0^\infty \frac{1}{\sqrt{ba}(u^2+1)}\,\mathrm{d}u$$
$$=\frac{1}{\sqrt{ba}}\arctan\frac{\sqrt{a}\omega}{\sqrt{b}}\Big|_0^\infty=\frac{\pi}{2\sqrt{ba}}.$$

For the induction step, recall the power reduction formula [21, page 82]

$$I_{(m,0)}=\int_0^\infty \frac{1}{(a\omega^2+b)^m}\mathrm{d}\omega=\frac{\omega}{2b(m-1)\,(a\omega^2+b)^{m-1}}\Big|_0^\infty$$
$$+\frac{2m-3}{2b(m-1)}\int_0^\infty \frac{1}{(a\omega^2+b)^{m-1}}\mathrm{d}\omega=0+\frac{2m-3}{2b(m-1)}$$
$$\cdot\int_0^\infty \frac{1}{(a\omega^2+b)^{m-1}}\mathrm{d}\omega=\frac{\pi}{2}\frac{(2m-3)!!}{(2m-2)!!b^{\frac{2m-1}{2}}a^{\frac{1}{2}}}.$$

Then we compute the base case $(m,1)$:

$$I_{(m,1)}=\int_0^\infty \frac{\omega}{(a\omega^2+b)^m}\,\mathrm{d}\omega \overset{u=a\omega^2+b}{=} \int_b^\infty \frac{1}{2au^m}\,\mathrm{d}u$$
$$=-\frac{1}{2a(m-1)u^{m-1}}\Big|_b^\infty=\frac{1}{2(m-1)b^{m-1}a}.$$

Suppose (35) holds for $(m-1,n)$. We use integration by parts to calculate $I_{(m,n+2)}$, i.e., $\int u\mathrm{d}v=uv-\int v\mathrm{d}u$. Let $u=\omega^{n+1}$, $v=-\frac{1}{2a(m-1)(a\omega^2+b)^{m-1}}$, $\mathrm{d}v=\frac{\omega\,\mathrm{d}\omega}{(a\omega^2+b)^m}$,

$$I_{(m,n+2)}=\int_0^\infty \frac{\omega^{n+2}}{(a\omega^2+b)^m}\,\mathrm{d}\omega=\frac{n+1}{2a(m-1)}I_{(m-1,n)}$$
$$-\frac{\omega^{n+1}}{2a(m-1)(a\omega^2+b)^{m-1}}\Big|_0^\infty=0+\frac{n+1}{2a(m-1)}I_{(m-1,n)}.$$

The solutions to this recurrence relation using the base cases $(m-1,0)$ and $(m-1,1)$ as the initial conditions are $I_{(m,n+2)}=\frac{\pi}{2}\frac{(n+1)!!(2m-n-5)!!}{(2m-2)!!b^{\frac{2m-n-3}{2}}a^{\frac{n+3}{2}}}$ and $I_{(m,n+2)}=\frac{(n+1)!!(2m-n-5)!!}{(2m-2)!!b^{\frac{2m-n-3}{2}}a^{\frac{n+3}{2}}}$ for n even and odd, respectively, which equals (35) for $(m,n+2)$ for all possible values of n. □

Lemma 3 provides explicit integral formulas to facilitate the derivation of $\mathcal{H}_2$ error bounds.

Lemma 4. *Let $f(\omega)$ be defined as in (26) for a collection of poles $\{p_i\}_{i=1}^m\subset\mathcal{K}$. Define a collection of related poles $p_i^*=\mathrm{Im}(p_i)+j\mathrm{Re}(p_i)=:p_i^y+jp_i^x$ and their conjugates $p_{m+i}^*:=\bar{p}_i^*$ for all $i\in I_m$. Choose constants c_i^* by (28). Then*

$$\int_{-\infty}^\infty f^4(\omega)\mathrm{d}\omega=\int_{-\infty}^\infty \frac{1}{\prod_{i=1}^m|j\omega-p_i|^4}\mathrm{d}\omega$$
$$=2\pi\sum_{i=1}^m\left(\frac{|c_i^*|^2}{-p_i^x}+\sum_{k=i+1}^m 4\mathrm{Im}\left(\frac{c_i^*\bar{c}_k^*}{p_i^*-\bar{p}_k^*}\right)\right)\equiv\alpha_m. \tag{36}$$

Proof of Lemma 4: We first decompose denominators of $f^2(\omega)$ in the complex domain, and then leverage the proved partial fraction decomposition to redefined poles.

$$f^2(\omega)=\frac{1}{\prod_{i=1}^m((\omega-p_i^y)^2+(p_i^x)^2)}$$
$$=\frac{1}{\prod_{i=1}^m(\omega-(p_i^y+p_i^xj))(\omega-(p_i^y-p_i^xj))}$$
$$\overset{p_i^*=p_i^y+p_i^xj}{=}\frac{1}{\prod_{i=1}^m(\omega-p_i^*)(\omega-\bar{p}_i^*)}\overset{\substack{\text{rewrite }\bar{p}_i^*\\ \text{subscript}}}{=}\frac{1}{\prod_{i=1}^{2m}(\omega-p_i^*)}$$
$$\overset{(29)}{=}\sum_{i=1}^{2m}c_i^*\frac{1}{\omega-p_i^*}. \tag{37}$$

Note that $c_{i+m}^*=\bar{c}_i^*$ for all $i\in I_m$ by (28). Let $\omega-p_i^*=r_i^*e^{j\theta_i}$ for all $i\in I_m$. Since ω is real so $\omega-\bar{p}_i^*=\overline{\omega-p_i^*}$ for all $i\in I_m$.

Since all poles lie in the open left half plane, $p_i^x<0$, the imaginary part of $\omega-p_i^*$ will always be positive for $1\leq i\leq m$. As $p_k^*=\bar{p}_{k-m}^*$ for all $m+1\leq k\leq 2m$, the imaginary part of $\omega-p_k^*$ will always be negative for $m+1\leq k\leq 2m$. Thus, as $\omega\to+\infty$, $\theta_i\to 0$ for $1\leq i\leq m$ and $\theta_k\to 2\pi$ for $m+1\leq k\leq 2m$. In addition, as $\omega\to-\infty$, $\theta_i\to\pi$ and $\theta_k\to\pi$ for all $1\leq i\leq m$ and $m+1\leq k\leq 2m$.

Using the partial fraction decomposition, we compute

$$f^4(\omega)=\frac{1}{\prod_{i=1}^m|j\omega-p_i|^4}\overset{(37)}{=}\left(\sum_{i=1}^{2m}c_i^*\frac{1}{\omega-p_i^*}\right)^2$$
$$=\sum_{i=1}^{2m}\left(\frac{(c_i^*)^2}{(\omega-p_i^*)^2}+2\sum_{k=i+1}^{2m}\frac{c_i^*c_k^*}{(\omega-p_i^*)(\omega-p_k^*)}\right)$$
$$=\sum_{i=1}^{2m}\left(\frac{(c_i^*)^2}{(\omega-p_i^*)^2}+2\sum_{k=i+1}^{2m}\frac{c_i^*c_k^*}{p_i^*-p_k^*}\left(\frac{1}{\omega-p_i^*}-\frac{1}{\omega-p_k^*}\right)\right)$$
$$=\sum_{i=1}^{2m}\frac{(c_i^*)^2}{(\omega-p_i^*)^2}+2\sum_{i=1}^{2m}\sum_{k=i+1}^{2m}\frac{c_i^*c_k^*}{p_i^*-p_k^*}\left(\frac{1}{\omega-p_i^*}-\frac{1}{\omega-p_k^*}\right)$$

Now we simplify the integral of square terms and product terms separately. It's straightforward to show $(c_i^*)^2$ and $(\bar{c}_i^*)^2$ are complex conjugates since c_i^* and $\bar{c}_i^*$ are complex conjugates for all $i\in I_m$. Suppose $(c_i^*)^2=a_i+b_ij$, and $(\bar{c}_i^*)^2=a_i-b_ij$, where $a_i=\mathrm{Re}((c_i^*)^2), b_i=\mathrm{Im}((c_i^*)^2)$.

Since the calculus method still applies to complex numbers. The integral of the first term will be

$$\int_{-\infty}^\infty\sum_{i=1}^{2m}\frac{(c_i^*)^2}{(\omega-p_i^*)^2}\mathrm{d}\omega=\sum_{i=1}^{2m}\int_{-\infty}^\infty\frac{(c_i^*)^2}{(\omega-p_i^*)^2}$$
$$=\sum_{i=1}^{2m}\frac{(c_i^*)^2}{\omega-p_i^*}\Big|_{-\infty}^\infty=0. \tag{38}$$

The integral of the second term will be

$$\int_{-\infty}^\infty 2\sum_{i=1}^{2m}\sum_{k=i+1}^{2m}\frac{c_i^*c_k^*}{p_i^*-p_k^*}\left(\frac{1}{\omega-p_i^*}-\frac{1}{\omega-p_k^*}\right)\mathrm{d}\omega$$
$$=2\sum_{i=1}^{2m}\sum_{k=i+1}^{2m}\frac{c_i^*c_k^*}{p_i^*-p_k^*}\ln\frac{(\omega-p_i^*)}{(\omega-p_k^*)}\Big|_{-\infty}^\infty$$
$$=2\left(\sum_{i=1}^{m}\sum_{k=i+1}^{m}\bullet+\sum_{i=m+1}^{2m}\sum_{k=i+1}^{2m}\bullet+\sum_{i=1}^{m}\sum_{k=m+1}^{2m}\bullet\right)\equiv 2\Sigma. \tag{39}$$

We compute

$$\ln\frac{(\omega-p_i^*)}{(\omega-p_k^*)}\Big|_{-\infty}^\infty=\ln\left|\frac{(\omega-p_i^*)}{(\omega-p_k^*)}\right|e^{j(\theta_i-\theta_k)}\Big|_{-\infty}^\infty$$

$$= \ln\left|\frac{(\omega - p_i^*)}{(\omega - p_k^*)}\right|\Bigg|_{-\infty}^{\infty} + \ln e^{j(\theta_i - \theta_k)}\Big|_{-\infty}^{\infty} = 0 + j(\theta_i - \theta_k)|_{-\infty}^{\infty}$$

$$= \begin{cases} -2\pi j & 1 \le i \le m, m+1 \le k \le 2m \\ 0 & 1 \le i, k \le m \text{ or } m+1 \le i, k \le 2m \end{cases}. \tag{40}$$

Define $c_{ik}^* = \frac{c_i^* c_k^*}{p_i^* - p_k^*}$. Then for any $1 \le i \le m$ and $m+1 \le k \le 2m$ with $k \ne i+m$, the contribution to the above sum from the poles p_i^*, p_k^* and their conjugates is:

$$c_{ik}^*(-2\pi j) + \bar{c}_{ik}^*(2\pi j)$$
$$= c_{ik}^*(-2\pi j) + \overline{c_{ik}^*(-2\pi j)} = 2\mathrm{Re}(c_{ik}^*(-2\pi j)) = 4\pi \mathrm{Im}(c_{ik}^*).$$

Furthermore, for any $1 \le i \le m$ and $k = i+m$, the contribution to the above sum from the pole p_i and its conjugates is:

$$c_{ik}^*(-2\pi j)$$
$$= \frac{c_i^* \bar{c}_i^*}{p_i^* - \bar{p}_i^*}(-2\pi j) = \frac{|c_i|^2}{2j\mathrm{Im}(p_i)}(-2\pi j) = \pi \frac{|c_i|^2}{-p_i^x}.$$

Combining the above with (39) yields the desired result. □

Lemma 5. *Define the indicator function $\mathcal{I}(k)$ to be 1 when k is even and 0 when k is odd. Let $\Gamma_m^k = \left(\frac{k}{2}+1\right)^2 \mathcal{I}(k) + 2\sum_{j=1}^{\lfloor (k+1)/2 \rfloor} j(m - |m-2+j-k|)$. Then*

$$\left(\sum_{k=0}^{m-1} \omega^k\right)^4 = \Gamma_m^{2m-2}\omega^{2m-2} + \sum_{k=0}^{2m-3} \Gamma_m^k(\omega^k + \omega^{4m-4-k}). \tag{41}$$

Proof of Lemma 5: First, we observe that the coefficients of ω^k and ω^{4m-4-k} are equal for all $k \in \{0, \dots, 2m-3\}$. This symmetry allows us to derive only the coefficients for $k \in \{0, \dots, 2m-2\}$, since the other coefficients will be identical to these [22].

We begin by considering the square of the sum

$$\left(\sum_{k=0}^{m-1} \omega^k\right)^2 = \underbrace{\sum_{i=0}^{m-2}(i+1)\omega^i}_{\Sigma_1} + \underbrace{\sum_{j=m-1}^{2m-2}(2m-1-j)\omega^j}_{\Sigma_2}. \tag{42}$$

We will compute the coefficient of each ω^k in $(\sum_{k=0}^{m-1}\omega^k)^4$ for $k \in \{0, \dots, 2m-2\}$ by squaring the expression for $(\sum_{k=0}^{m-1}\omega^k)^2$ given by (42).

First consider k even. Some terms in the coefficient of ω^k arise as the squares of monomials from (42). As $k \le 2m-2$, such terms can only arise as the squares of monomials from Σ_1. Furthermore, only the monomial $\omega^{k/2}$ has as its square ω^k. Thus, the contribution of this term to the coefficient of ω^k is $(k/2+1)^2$.

The other terms in the coefficient of ω^k arise from cross products between monomials in (42) of different powers. As the product of two different monomials from Σ_2 always has an exponent greater than or equal to $2m-1 > k$, the terms in the coefficient of ω^k can only arise as the product of one monomial from Σ_1 and one monomial from Σ_2, or from the product of two different monomials from Σ_1.

To distinguish these two cases, define $k_1 := \max\{0, k-m+2\}$. Any such product will involve two monomials - let i and j be their respective exponents, and note that we must have $i+j=k$ for this product to contribute to the coefficient of ω^k.

For any $i \in \{0, \dots, k_1-1\}$, $j = k-i \ge k-(k_1-1) = m-1$ so the monomial with exponent j must belong to Σ_2, which implies that the monomial with exponent i must belong to Σ_1 in this case. Thus, this contribution is given by:

$$2\sum_{j=1}^{k_1} j(2m-2+j-k).$$

For any $i \in \{k_1, \dots, k/2-1\}$, $i \le k/2-1 \le (2m-2)/2-1 = m-2$. Also, $i \ge k_1 \ge k-(m-2)$ so $j = k-i \le k-k_1 = m-2$. Thus, both monomials must belong to Σ_2 in this case. Thus, this contribution is given by:

$$2\sum_{j=k_1+1}^{k/2} j(2-j+k).$$

Therefore, the coefficient of the term ω^k is given by the sum of the square term and the two cross product cases above as:

$$2\sum_{j=1}^{k_1} j(2m-2+j-k) + 2\sum_{j=k_1+1}^{k/2} j(2-j+k)$$
$$+ \left(\frac{k}{2}+1\right)^2 = 2\sum_{j=1}^{k/2} j(m - |m-2+j-k|) + \left(\frac{k}{2}+1\right)^2.$$

For odd k, the analysis simplifies: there is no square term, and the calculation for the cross products follows an analogous argument to that in the even case. Combining the odd and even cases for k yields the coefficient Γ_m^k. □

Corollary 3 provides an approximation error bound for a single repeated pole in the SISO case.

Corollary 3. *Let $p_1, \dots, p_m, q \in \mathcal{K}$, and $\mathcal{P} = \cup_{i=1}^m p_i$, let $\hat{d}(q) = \max_i |p_i - q|$. Let $s = j\omega$ for some $\omega \in \mathbb{R}$. Then there exist constants $c_1, \dots, c_m \in \mathbb{C}$ and $k_\bullet^{(p,q,m)} > 0$ for each $\bullet \in \{2, \infty\}$ such that*

$$\left\|\sum_{i=1}^m c_i \frac{1}{s-p_i} - \frac{1}{(s-q)^m}\right\|_{\mathcal{H}_\bullet} \le k_\bullet^{(p,q,m)}\hat{d}(q). \tag{43}$$

Proof of Corollary 3: Now we can derive an upper bound for $\int_{-\infty}^{\infty} g^4(\omega)\mathrm{d}\omega$ from (26) using Lemmas 2, 3, and 5

$$\int_{-\infty}^{\infty} g^4(\omega)\mathrm{d}\omega \overset{(33)}{\le} \int_{-\infty}^{\infty} \frac{(\sum_{k=0}^{m-1}|\omega|^k)^4}{(a\omega^2+b)^{2m}}\mathrm{d}\omega$$
$$= 2\int_0^{\infty} \frac{(\sum_{k=0}^{m-1}\omega^k)^4}{(a\omega^2+b)^{2m}}\mathrm{d}\omega \overset{(41)}{=} 2\Big(\Gamma_m^{2m-2}$$
$$\cdot \int_0^{\infty} \frac{\omega^{2m-2}}{(a\omega^2+b)^{2m}}\mathrm{d}\omega + \sum_{k=0}^{2m-3}\Gamma_m^k \int_0^{\infty} \frac{\omega^k + \omega^{4m-4-k}}{(a\omega^2+b)^{2m}}\mathrm{d}\omega\Big)$$
$$\overset{(35)}{=} 2\Big(\Gamma_m^{2m-2} I_{(2m,2m-2)}$$
$$+ \sum_{k=0}^{2m-3}\Gamma_m^k \left(I_{(2m,k)} + I_{(2m,4m-4-k)}\right)\Big) \equiv \beta_m. \tag{44}$$

We first consider the $\mathcal{H}_2$ case. Let c.s. denote the Cauchy-Schwarz inequality. Then by Lemma 4 we have

$$\begin{aligned}
\left\|\sum_{i=1}^{m} c_i \frac{1}{s-p_i} - \frac{1}{(s-q)^m}\right\|_{\mathcal{H}_2} &\overset{(26)}{\leq} \sqrt{\frac{1}{2\pi}\int_{-\infty}^{\infty} f^2(\omega)g^2(\omega)\mathrm{d}\omega} \\
&\quad \cdot ((|q|+2)^m - (|q|+1)^m)\ell(\mathcal{K})^{m-1}\hat{d}(q) \\
&\overset{\text{c.s.}}{\leq} \frac{1}{\sqrt{2\pi}}\left(\int_{-\infty}^{\infty} f^4(\omega)\mathrm{d}\omega \int_{-\infty}^{\infty} g^4(\omega)\mathrm{d}\omega\right)^{\frac{1}{4}} \\
&\quad \cdot ((|q|+2)^m - (|q|+1)^m)\ell(\mathcal{K})^{m-1}\hat{d}(q) \\
&\overset{(36)(44)}{\leq} \frac{(\alpha_m\beta_m)^{\frac{1}{4}}((|q|+2)^m - (|q|+1)^m)\ell(\mathcal{K})^{m-1}}{\sqrt{2\pi}}\hat{d}(q) \\
&\equiv k_2^{(p,q,m)}\hat{d}(q).
\end{aligned}$$

To analyze the $\mathcal{H}_\infty$ norm, we first observe that the supremum of $g(\omega)$ is invariant under sign reversal of q_y. Let $q_y^+ = |q_y| \geq 0$ and $q_y^- = -|q_y| \leq 0$, and let $g(q_y^+, \omega)$ and $g(q_y^-, \omega)$ denote the values of $g(\omega)$ for $q_y = q_y^+$ and $q_y = q_y^-$, respectively. Then

$$\begin{aligned}
g(q_y^-, \omega) &= \frac{\sum_{k=0}^{m-1}|\omega|^k}{((\omega - q_y^-)^2 + q_x^2)^{m/2}} = \frac{\sum_{k=0}^{m-1}|\omega|^k}{((\omega + q_y^+)^2 + q_x^2)^{m/2}} \\
&= \frac{\sum_{k=0}^{m-1}|-\omega|^k}{((-\omega - q_y^+)^2 + q_x^2)^{m/2}} = g(q_y^+, -\omega).
\end{aligned}$$

Thus $\sup_{\omega\in\mathbb{R}} g(\omega)(q_y^-, \omega) = \sup_{\omega\in\mathbb{R}} g(\omega)(q_y^+, \omega)$.

Without loss of generality, we assume $q_y \geq 0$, then

$$\begin{aligned}
&\left\|\sum_{i=1}^{m} c_i \frac{1}{s-p_i} - \frac{1}{(s-q)^m}\right\|_{\mathcal{H}_\infty} \\
&\overset{(26)}{\leq} ((|q|+2)^m - (|q|+1)^m)\ell(\mathcal{K})^{m-1}\hat{d}(q)\sup_{\omega\in\mathbb{R}} f(\omega)g(\omega) \\
&\overset{\text{c.s.}}{\leq} ((|q|+2)^m - (|q|+1)^m)\ell(\mathcal{K})^{m-1}\hat{d}(q)\sup_{\omega\in\mathbb{R}} f(\omega)\sup_{\omega\in\mathbb{R}} g(\omega) \\
&\leq \frac{((|q|+2)^m - (|q|+1)^m)\ell(\mathcal{K})^{m-1}}{\prod_{i=1}^{m}(-p_i^x)}\sup_{\omega\in\mathbb{R}} g(\omega)\hat{d}(q). \qquad (45)
\end{aligned}$$

Next we show that $\sup_{\omega\in\mathbb{R}} g(\omega)$ achieves a maximum at some $\omega > 0$. To see this, first observe that for any $\omega > 0$, we have $g(q_y, \omega) > g(q_y, -\omega)$, since the numerator $\sum_{k=0}^{m-1}|\omega|^k$ remains unchanged under sign reversal, while the denominator increases due to the inequality $(-\omega - q_y)^2 + q_x^2 \geq (\omega - q_y)^2 + q_x^2$, so $\sup_{\omega\in\mathbb{R}} g(\omega) = \sup_{\omega\geq 0} g(\omega)$. Since $g(q_y, 0) = 0$, $\lim_{\omega\to\infty} g(q_y, \omega) = 0$, $g(q_y, \omega) > 0$ for all $\omega > 0$, and g is continuous, its supremum must be attained at some finite maximum $\omega^* > 0$. Thus, $g(q_y, \omega^*) = \frac{\sum_{k=0}^{m-1}(\omega^*)^k}{((\omega^*-q_y)^2+q_x^2)^{m/2}}$.

Thus, to bound the $\mathcal{H}_\infty$ norm from (45) it suffices to bound the maximum of the function $h(\omega) := \frac{\sum_{k=0}^{m-1}\omega^k}{((\omega-q_y)^2+q_x^2)^{m/2}} = \frac{1-\omega^m}{(1-\omega)((\omega-q_y)^2+q_x^2)^{m/2}}$ for $\omega > 0$. Our goal is to bound the maximum of this function. As $h(\omega)$ achieves its global maximum in the interior of its domain, its derivative $h'(\omega)$ at this maximum must be zero. Thus, our goal is to bound this global maximum by bounding the region containing the roots of its derivative $h'(\omega)$. Differentiating, we obtain

$$\begin{aligned}
h'(\omega) =& \frac{((m-1)\omega^m - m\omega^{m-1} + 1)((\omega - q_y)^2 + q_x^2)}{(1-\omega)^2((\omega - q_y)^2 + q_x^2)^{m/2+1}} \\
&- \frac{(1-\omega^m)(1-\omega)m(\omega - q_y)}{(1-\omega)^2((\omega - q_y)^2 + q_x^2)^{m/2+1}}.
\end{aligned}$$

To identify the local optima, we set $h'(\omega) = 0$, leading to the equation

$$\begin{aligned}
0 =& \omega^{m+2} + (m-2)q_y\omega^{m+1} - ((m-1)r + mq_y)\omega^m \\
&- mq_y + mr\omega^{m-1} - (m+1)\omega^2 + (mq_y + m + 2q_y)\omega - r
\end{aligned}$$

where $r = q_x^2 + q_y^2$. Denote the coefficient of ω^i in this polynomial by a_i for all $i \in \{0, \ldots, m+2\}$. Instead of finding the precise solutions for $h'(\omega) = 0$, we use Cauchy's root bound, which is sharper than Lagrange's bound in this situation and gives an upper bound for the magnitude of all roots of $h'(\omega)$ as $\hat{\omega} = 1 + \max_{i<m+2}|a_i| =$

$$1 + \max\{(m-1)r + mq_y, mr, m+1, mq_y + m + 2q_y\}. \qquad (46)$$

By the above discussion, $\max_{\omega>0} h(\omega) = \max_{\omega\in(0,\hat{\omega}]} h(\omega)$, so the $\mathcal{H}_\infty$ norm from (45) can be bounded by

$$\begin{aligned}
\left\|\sum_{i=1}^{m} c_i \frac{1}{s-p_i} - \frac{1}{(s-q)^m}\right\|_{\mathcal{H}_\infty} &\leq \frac{\max_{\omega\in(0,\hat{\omega}]} h(\omega)}{\prod_{i=1}^{m}(-p_i^x)} \\
&\quad \cdot ((|q|+2)^m - (|q|+1)^m)\ell(\mathcal{K})^{m-1}\hat{d}(q) \\
&\leq \frac{((|q|+2)^m - (|q|+1)^m)\ell(\mathcal{K})^{m-1}\hat{d}(q)\sum_{k=0}^{m-1}\hat{\omega}^k}{\prod_{i=1}^{m}(-p_i^x)\inf_{\omega>0}((\omega - q_y)^2 + q_x^2)^{m/2}} \\
&\leq \frac{((|q|+2)^m - (|q|+1)^m)\ell(\mathcal{K})^{m-1}\sum_{k=0}^{m-1}\hat{\omega}^k}{\prod_{i=1}^{m}(-p_i^x)(-q_x)^m}\hat{d}(q).
\end{aligned}$$

The case $q_y = 0$ is naturally included as a degeneration of this bound. □

Theorem 1 extends the approximation error bound to an arbitrary number of (possibly repeated) poles and to the MIMO case.

Proof of Theorem 1: Both the $\mathcal{H}_2$ and $\mathcal{H}_\infty$ error bounds in the MIMO case can be derived analogously to the $\mathcal{H}_\infty$ norm derivation in [11, Proof of Theorem 1], by appropriately substituting the error bounds from the SISO case as given in Corollary 3. □

Proofs of Theorems 2 and 3: The proofs follow analogous arguments to the proofs of [12, Theorem 2 and Theorem 3]. □

B. Proof of Theorem 4

The following corollary determines the maximum distance from any $q \in \mathcal{K}$ to the closest $p \in \mathcal{P}_n$ for the trapezoidal pole selection described in Section IV-A. Let $d(z, \mathcal{P}_n) = \inf_{p\in\mathcal{P}_n}|z - p|$.

Corollary 4. *Suppose the trapezoid pole selection $\mathcal{P}_n$ is constructed as in Section IV-A. Then, for any $z \in \mathcal{K}$,*

$$d(z, \mathcal{P}_n) \leq d_{\max} = \bar{l}\sqrt{13/4 + \lceil\tan\theta\rceil^2 + 3\lceil\tan\theta\rceil}.$$

Proof of Corollary 4: Since both the trapezoid $\mathcal{K}$ and the overlaid grid are symmetric with respect to the real axis, it suffices to consider only the upper half plane. For analysis, let k_a, k_b, and k_c denote half the height, half the length of the shorter base, and half the length of the longer base of $\mathcal{K}$,

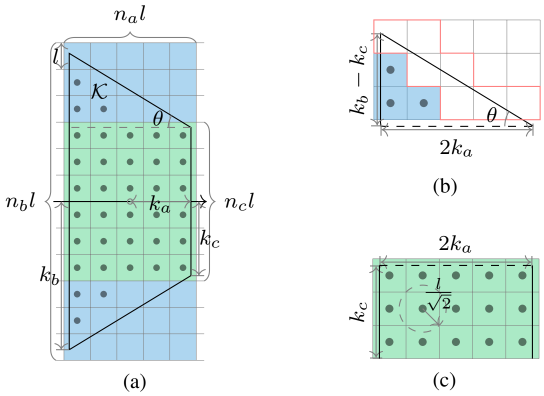

Fig. 3. Trapezoid pole selection geometric illustrations.

respectively, as shown in Fig. 3a. We consider a $n_b l \times n_a l$ grid with cell size l satisfying $l \le \bar{l} := \min\{k_a, k_c\}$, where $n_\bullet := \lfloor 2k_\bullet/l \rfloor$ for $\bullet \in \{a, b, c\}$. The upper half of $\mathcal{K}$ together with the grid can then be decomposed into a triangular region with $\frac{n_b - n_c}{2} l \times n_a l$ subgrid (see Fig. 3b) and a rectangular region (see Fig. 3c).

Consider any grid cell C that contains a pole from $\mathcal{P}_n$, but has no poles from $\mathcal{P}_n$ vertically above it. The maximum number of grid cells that intersect $\mathcal{K}$ and lie vertically above C is $\lceil \tan\theta \rceil + 1$.

Thus, for any $z \in \mathcal{K}$ that lies in a grid cell above C, the maximum distance from z to the pole in C is bounded by:

$$\begin{aligned} d_1 &= l\sqrt{(l/2 + (\lceil \tan\theta \rceil + 1)l)^2 + l^2} \\ &= l\sqrt{13/4 + \lceil \tan\theta \rceil^2 + 3\lceil \tan\theta \rceil}. \end{aligned}$$

Consider any $z \in \mathcal{K}$ that lies in a grid cell C that contains a pole in $\mathcal{P}_n$. Then the maximum distance from z to that pole, and hence to $\mathcal{P}_n$, is bounded by:

$$d_2 = \frac{l}{\sqrt{2}} \le d_1.$$

Combining the above cases implies that any $z \in \mathcal{K}$ is at most a distance d_1 away from $\mathcal{P}_n$.

This geometric decomposition ensures that every point in the trapezoidal region $\mathcal{K}$ lies within a distance $d_{\max}$ from this grid pole selection $\mathcal{P}_n$. □

Proof of Theorem 4: We derive an upper bound on the grid length l as a function of the number of poles $n(l)$ in the pole selection $\mathcal{P}_n$. Since the number of poles $n(l)$ is upper bounded by the number of all cells in the entire $n_b l \times n_a l$ grid yields $n(l) \le n_b \times n_a = (\lfloor 2k_a/l \rfloor)(\lfloor 2k_b/l \rfloor) \le (2k_a/l)(2k_b/l)$, which leads to an upperbound on l

$$0 < l \le \frac{2\sqrt{k_a k_b}}{\sqrt{n(l)}}. \tag{47}$$

Let $S \in \frac{1}{s}\mathcal{RH}_\infty$ and let $\mathcal{Q}$ be the poles of S. For any pole $q \in \mathcal{Q}$, by Theorem 4 the distance from q to its closest pole in the grid pole selection $\mathcal{P}_n$ is at most $d_{\max}$. By traversing along a path of neighboring poles in the grid, the cumulative increase in distance from q to each successive pole is bounded by increments of at most l, since all grid cells have the same length l. That is, the m_q closest poles in $\mathcal{P}_n$ to q are all within a distance of $(m_q - 1)l + d_{\max}$ from q.

Next we characterize the worst case approximating distance for grid pole selection. For any q lying in the compact set $\mathcal{K}$, suppose $p_{\hat{k}}$ and $p_{\hat{i}}$ are the closest and furthest poles in the collection of m_q closest approximating approximating poles $\mathcal{P}_{n(l)}(q)$ respectively, then the distance from $p_{\hat{k}}$ to $p_{\hat{i}}$ will be less than or equal to $(m_q - 1)l$ since each selected pole will have at least one neighboring pole in terms of l distance. Thus

$$\begin{aligned} \hat{d}(q) &= \max_{p \in \mathcal{P}_{n(l)}(q)} |p - q| = d(q, p_{\hat{i}}) \le d(q, p_{\hat{k}}) + d(p_{\hat{k}}, p_{\hat{i}}) \\ &\overset{\text{Corollary 4}}{\le} d_{\max} + (m_q - 1)\bar{l}. \end{aligned}$$

Since $d_{\max} \le \bar{l}\sqrt{13/4 + \lceil \tan\theta \rceil^2 + 3\lceil \tan\theta \rceil}$, the worst case approximation error over $\mathcal{Q}$ satisfies

$$\begin{aligned} D(\mathcal{P}_m) &= \max_{q \in \mathcal{Q}} \hat{d}(q) \le d_{\max} + (m_{\max} - 1)\bar{l} \\ &\le \left(\sqrt{13/4 + \lceil \tan\theta \rceil^2 + 3\lceil \tan\theta \rceil} + m_{\max} - 1\right)\bar{l} \\ &\overset{(47)}{\le} \frac{2(\sqrt{13/4 + \lceil \tan\theta \rceil^2 + 3\lceil \tan\theta \rceil} + m_{\max} - 1)\sqrt{k_a k_b}}{\sqrt{n(\bar{l})}}. \end{aligned}$$

this provides a bound on $D(\mathcal{P})$. □

Proof of Corollary 1: By Theorem 4, $\{p_n\}_{n=1}^\infty$ is a sequence of poles with geometric convergence rate $\frac{1}{n^{1/2}}$. Thus, the result follows from Theorem 3. □

C. Proof of Theorem 5

The key technical result required to prove Theorem 5 is Lemma 6, which extends the approximation error bounds of Theorem 1 to bound the error between a feasible solution (Φ_u, Φ_x) of (3) and the optimal solution (Φ_u^*, Φ_x^*) of (2).

Lemma 6. *let (Φ_x^*, Φ_u^*) denote the optimal solution to (2). Then there exist $\Phi_x, \Phi_u \in \frac{1}{s}\mathcal{RH}_\infty$ which are a feasible solution to (3), and constants $K_\infty^u, K_2^u, K_\infty^x, K_2^x > 0$, such that*

$$\begin{aligned} \|\Phi_u - \Phi_u^*\|_{\mathcal{H}_\infty} &\le K_\infty^u D(\mathcal{P}) \quad \|\Phi_u - \Phi_u^*\|_{\mathcal{H}_2} \le K_2^u D(\mathcal{P}) \\ \|\Phi_x - \Phi_x^*\|_{\mathcal{H}_\infty} &\le K_\infty^x D(\mathcal{P}) \quad \|\Phi_x - \Phi_x^*\|_{\mathcal{H}_2} \le K_2^x D(\mathcal{P}). \end{aligned}$$

Before presenting the proof of Lemma 6, we first establish several supporting lemmas.

Lemma 7. *Let k be any integer, m a nonnegative integer, and s be on the imaginary axis. Let $p_1, \dots, p_m, q \in \mathcal{K}$. Denote the diameter of $\mathcal{K}$ as $\ell(\mathcal{K})$. Let $\hat{d}(q) = \max_i |p_i - q|$, Suppose further that $m \ge k$ if m is positive or $m > k$ if $m = 0$. Then there exists $K > 0$ such that*

$$\left| \frac{(s-q)^k}{\prod_{i=1}^m (s - p_i)} - (s-q)^{k-m} \right| \le K\hat{d}(q). \tag{48}$$

and

$$\left\| \frac{(s-q)^k}{\prod_{i=1}^m (s - p_i)} - \frac{1}{(s-q)^{m-k}} \right\|_{\mathcal{H}_2} \le K\hat{d}(q). \tag{49}$$

Proof of Lemma 7: We compute

$$\begin{aligned}&\left|\frac{(s-q)^k}{\prod_{i=1}^m(s-p_i)}-(s-q)^{k-m}\right|\\&=\frac{|(s-q)^m-\prod_{i=1}^m(s-p_i)|}{|(s-q)^{m-k}\prod_{i=1}^m(s-p_i)|}\\&\overset{(32)}{\leq}\frac{((|q|+2)^m-(|q|+1)^m)\ell(\mathcal{K})^{m-1}\sum_{h=0}^{m-1}|s|^h}{|s-q|^{m-k}\prod_{i=1}^m|s-p_i|}\hat{d}(q),\end{aligned}\tag{50}$$

denote $f(s)=\frac{((|q|+2)^m-(|q|+1)^m)\ell(\mathcal{K})^{m-1}\sum_{h=0}^{m-1}|s|^h}{|s-q|^{m-k}\prod_{i=1}^m|s-p_i|}$.

If $s=j\omega$, and k satisfies the given assumptions then by Lemma 2 we have

$$\begin{aligned}f(s)&=\frac{((|q|+2)^m-(|q|+1)^m)\ell(\mathcal{K})^{m-1}}{|j\omega-q|^{m-k}}\frac{\sum_{h=0}^{m-1}|\omega|^h}{\prod_{i=1}^m|j\omega-p_i|}\\&\overset{(33)}{\leq}\frac{((|q|+2)^m-(|q|+1)^m)\ell(\mathcal{K})^{m-1}}{(-q_x)^{m-k}}\frac{\sum_{h=0}^{m-1}|\omega|^h}{(a\omega^2+b)^{m/2}}.\end{aligned}$$

Without loss of generality it suffices to consider the case where $q_y>0$. By an analogous argument as in the proof of Corollary 3, in this case the supremum of $f(j\omega)$ is attained at a finite maximum, and this maximum can be bounded as

$$\frac{\sum_{h=0}^{m-1}\omega^h}{(a\omega^2+b)^{m/2}}\leq\frac{\sum_{h=0}^{m-1}\hat{\omega}^h}{b^{\frac{m}{2}}}$$

where $\hat{\omega}$ is defined in (46), Then (48) follows after defining $K=\frac{((|q|+2)^m-(|q|+1)^m)\ell(\mathcal{K})^{m-1}\sum_{h=0}^{m-1}\hat{\omega}^h}{(-q_x)^{m-k}b'^{\frac{m}{2}}}$.

By (50), we obtain

$$\begin{aligned}&\left\|\frac{(s-q)^k}{\prod_{i=1}^m(s-p_i)}-\frac{1}{(s-q)^{m-k}}\right\|_{\mathcal{H}_2}\overset{(50)}{\leq}\hat{d}(q)((|q|+2)^m\\&-(|q|+1)^m)\ell(\mathcal{K})^{m-1}\left\|\frac{1}{|j\omega-q|^{m-k}}\frac{\sum_{h=0}^{m-1}|\omega|^h}{\prod_{i=1}^m|j\omega-p_i|}\right\|_{\mathcal{H}_2}.\end{aligned}\tag{51}$$

Therefore, it suffices to analyze the $\mathcal{H}_2$ norm of the last expression and subsequently multiply it by the remaining terms. When $m>k$, by Lemmas 2, 3, and 5

$$\begin{aligned}&\left\|\frac{1}{|j\omega-q|^{m-k}}\frac{\sum_{h=0}^{m-1}|\omega|^h}{\prod_{i=1}^m|j\omega-p_i|}\right\|_{\mathcal{H}_2}\\&\overset{(33)}{\leq}\sqrt{\frac{1}{2\pi}\int_{-\infty}^{\infty}\frac{1}{(a'\omega^2+b')^{m-k}}\frac{(\sum_{h=0}^{m-1}|\omega|^h)^2}{(a\omega^2+b)^m}\mathrm{d}\omega}\\&\overset{\text{c.s.}}{\leq}\frac{1}{\sqrt{2\pi}}\sqrt[4]{\int_{-\infty}^{\infty}\frac{1}{(a'\omega^2+b')^{2m-2k}}\mathrm{d}\omega\int_{-\infty}^{\infty}\frac{(\sum_{h=0}^{m-1}\omega^h)^4}{(a\omega^2+b)^{2m}}\mathrm{d}\omega}\\&\overset{(35)}{\leq}\frac{1}{\sqrt{2\pi}}\left(2I_{(2m-2k,0)}^{(a',b')}\right)^{\frac{1}{4}}\left(2\int_0^{\infty}\frac{(\sum_{h=0}^{m-1}\omega^h)^4}{(a\omega^2+b)^{2m}}\mathrm{d}\omega\right)^{\frac{1}{4}}\\&\overset{(41)(35)}{\leq}\frac{1}{\sqrt{\pi}}(I_{(2m-2k,0)}^{(a',b')}(\Gamma_m^{2m-2}I_{(2m,2m-2)}^{(a,b)}\\&+\sum_{k=0}^{2m-3}\Gamma_m^k(I_{(2m,k)}^{(a,b)}+I_{(2m,4m-4-k)}^{(a,b)})))^{\frac{1}{4}}=K'.\end{aligned}$$

When $m=k\geq1$,

$$\begin{aligned}&\left\|\frac{1}{|j\omega-q|^{m-k}}\frac{\sum_{h=0}^{m-1}|\omega|^h}{\prod_{i=1}^m|j\omega-p_i|}\right\|_{\mathcal{H}_2}\\&\overset{(33)}{\leq}\sqrt{\frac{1}{\pi}\int_0^{\infty}\frac{(\sum_{h=0}^{m-1}\omega^h)^2}{(a\omega^2+b)^m}\mathrm{d}\omega}\\&\overset{(42)}{=}\sqrt{\frac{1}{\pi}\int_0^{\infty}\frac{\sum_{i=0}^{m-2}(i+1)(\omega^i+\omega^{2m-2-i})+m\omega^{m-1}}{(a\omega^2+b)^m}\mathrm{d}\omega}\\&\overset{(35)}{=}\sqrt{\frac{\sum_{i=0}^{m-2}(i+1)(I_{(m,i)}^{(a,b)}+I_{(m,2m-2-i)}^{(a,b)})+mI_{(m,m-1)}^{(a,b)}}{\pi}}\\&\equiv K'.\end{aligned}$$

When $m=0>k$, $\left\|\frac{1}{|j\omega-q|^{m-k}}\right\|_{\mathcal{H}_2}\overset{(35)}{\leq}\sqrt{\frac{1}{\pi}I_{(2m-2k,0)}^{(a',b')}}\equiv K'$. Define $K=K'((|q|+2)^m-(|q|+1)^m)\ell(\mathcal{K})^{m-1}$, and then (51) yields the upper bound in (49). $\square$

Corollary 5 will help bound the error between the optimal and approximating transfer functions in terms of $D(\mathcal{P})$.

Corollary 5. *Let k be a nonnegative integer, m a positive integer. Let $q,\lambda,p_1,\ldots,p_m\in\mathcal{K}$ with $d\left(\lambda,\{p_i\}_{i=1}^m\right)\geq\delta>0$ and $d(\lambda,q)\geq\eta>0$. Let J be an elementary Jordan block. Denote the diameter of $\mathcal{K}$ as $\ell(\mathcal{K})$. Choose constants c_{p_i} as in (28). Then there exists $K>0$ such that*

$$\left\|\sum_{i=1}^m c_{p_i}(p_i-q)^m J(\lambda-p_i)^{-1}\frac{1}{s-p_i}\right\|_{\mathcal{H}_2}\leq K\hat{d}(q).\tag{52}$$

Proof of Corollary 5: First we derive a uniform upper bound of the spectral norm of the term inside the $\mathcal{H}_2$ norm in (52) for all s on the imaginary axis. By [12, Fact 1], it suffices to show that for each $l\in\{0,\ldots,m_q-1\}$ there exists $k_l>0$ such that the lth superdiagonal of the matrix in this term satisfies

$$\left|\sum_{i=1}^m c_{p_i}(p_i-q)^m(-1)^l(\lambda-p_i)^{-(l+1)}\frac{1}{s-p_i}\right|\leq k_l\hat{d}(q).$$

We derive this bound by following an analogous argument to the proof of [12, Corollary 2(b)], wher a_n and a_0 are constants that satisfy $|1-a_0|\leq K_0'\hat{d}(q)$ and $|a_n|\leq K_n'\hat{d}(q)$. We compute

$$\begin{aligned}&\left|\sum_{i=1}^m c_{p_i}(p_i-q)^m(-1)^l(\lambda-p_i)^{-(l+1)}\frac{1}{s-p_i}\right|\\&\overset{\text{[12, Proof of Corollary 2(b)]}}{\leq}\left|\frac{(s-q)^m}{\prod_{i=1}^m(s-p_i)}-1\right||\lambda-s|^{-l-1}+\frac{|1-a_0|}{|\lambda-s|^{l+1}}\\&\quad+\sum_{n=1}^{l}\frac{|a_n|}{|s-\lambda|^{l+1-n}}\\&\overset{s=j\omega,\ \text{Lemma 7}}{\leq}\left(\frac{((|q|+2)^m-(|q|+1)^m)\ell(\mathcal{K})^{m-1}}{(-\lambda_x)^{l+1}}\frac{\sum_{h=1}^m|\omega|^{m-h}}{\prod_{i=1}^m|j\omega-p_i|}\right.\\&\quad\left.+\frac{K_0'}{|j\omega-\lambda|^{l+1}}+\sum_{n=1}^{l}\frac{K_n'}{|j\omega-\lambda|^{l+1-n}}\right)\hat{d}(q).\end{aligned}\tag{53}$$

Take the $\mathcal{H}_2$ norm of both sides of (53) and apply the triangle inequality to isolate each term,

$$\begin{aligned}
&\left\|\sum_{i=1}^{m} c_{p_i}\left(p_i-q\right)^m(-1)^l\left(\lambda-p_i\right)^{-(l+1)} \frac{1}{s-p_i}\right\|_{\mathcal{H}_2} \\
&\overset{\substack{\text{triangle}\\\text{inequality}\\(53)}}{\leq}\left(\left\|\frac{((|q|+2)^m-(|q|+1)^m)\ell(\mathcal{K})^{m-1}}{(-\lambda_x)^{l+1}}\right.\right. \\
&\left.\left.\cdot\frac{\sum_{h=1}^m|\omega|^{m-h}}{\prod_{i=1}^m|j\omega-p_i|}\right\|_{\mathcal{H}_2}+\sum_{n=0}^{l}\left\|\frac{K_n'}{|j\omega-\lambda|^{l+1-n}}\right\|_{\mathcal{H}_2}\right)\hat{d}(q) \\
&\overset{\text{Lemma 7}}{\leq}\left(K+\sum_{n=0}^{l}K_n'\left\|\frac{1}{|j\omega-\lambda|^{l+1-n}}\right\|_{\mathcal{H}_2}\right)\hat{d}(q) \\
&\overset{\text{Lemma 2, 3}}{\leq}\left(K+\sum_{n=0}^{l}K_n'K\right)\hat{d}(q)\equiv K_l^*\hat{d}(q). \qquad (54)
\end{aligned}$$

Thus

$$\begin{aligned}
&\left\|\sum_{i=1}^{m} c_{p_i}\left(p_i-q\right)^m J\left(\lambda-p_i\right)^{-1} \frac{1}{s-p_i}\right\|_{\mathcal{H}_2} \\
&=\sqrt{\frac{1}{2\pi}\int_{-\infty}^{\infty}\|\sum_{i=1}^{m} c_{p_i}\left(p_i-q\right)^m J\left(\lambda-p_i\right)^{-1}\frac{1}{s-p_i}\|_F^2\mathrm{d}\omega} \\
&=\sqrt{\sum_{l=0}^{m_q-1}(m_q-l)\left\|\sum_{i=1}^{m}c_{p_i}\frac{(-1)^l(p_i-q)^m}{(\lambda-p_i)^{(l+1)}(s-p_i)}\right\|_{\mathcal{H}_2}^2} \\
&\overset{(54)}{\leq}\sqrt{\sum_{l=0}^{m_q-1}(m_q-l)K_l^{*2}\hat{d}(q)}\equiv K\hat{d}(q)
\end{aligned}$$

which completes the proof. □

Now we have prepared everything for proving Lemma 6.

Proof of Lemma 6: The intuition of the proof is to first select an optimal solution (Φ_x^*, Φ_u^*) to (2), and then select $\Phi_u(s)$ to approximate $\Phi_u^*(s)$, which yields (norm bound) by Theorem 1. $\|\Phi_u(s)-\Phi_u^*(s)\|_\bullet \leq K_\bullet^u D(\mathcal{P})$ immediately by constructing $\Phi_u(s)$ as Theorem 1. Next $\Phi_x(s)$ is defined as the unique solution to the SLS constraint in (3b), then we will show that Φ_x is a feasible solution to (14), and that it satisfies the approximation error bounds $\|\Phi_x(s)-\Phi_x^*(s)\|_\bullet \leq K_\bullet^x D(\mathcal{P})$. The main difference in the derivation compared to the discrete-time case in [12] is to show the bound $\|\Phi_x - \Phi_x^*\|_{\mathcal{H}_2} \leq K_2^x D(\mathcal{P})$. According to the proof of [12, Lemma 2], let $q \in \mathcal{Q}$ be the poles of $\Phi_x^*(s)$, λ be any stable plant pole, denote the error bounds are discussed separately for the cases $q \neq \lambda$ and $q = \lambda$.

Case 1: $q \neq \lambda$,

$$\begin{aligned}
&\|\Phi_x(s)-\Phi_x^*(s)\|_{\mathcal{H}_2} \\
&\overset{\substack{[12,\text{ Proof of}\\\text{Lemma 2]}}}{\leq}\sum_{i=1}^{m}\sum_{l=1}^{i}\|G_{(l,i)}^*\|_F\left\|\frac{(s-q)^{i-l}}{\prod_{j=1}^{i}(s-p_j^i)}-\frac{1}{(s-q)^l}\right\|_{\mathcal{H}_2} \\
&+\sum_{i=1}^{m}\|G_{(1,i)}^*\|_F\left\|\sum_{j=1}^{i}c_j^i\left(p_j^i-q\right)^i J\left(\lambda-p_j^i\right)^{-1}\frac{1}{s-p_j^i}\right\|_{\mathcal{H}_2} \\
&\overset{\substack{\text{Lemma 7}\\\text{Corollary 5}}}{\leq}\sum_{i=1}^{m}\sum_{l=1}^{i}\|G_{(l,i)}^*\|_F K_{(i,i-l)}^{(p^i,q)}\hat{d}(q) \\
&\quad+\sum_{i=1}^{m}\|G_{(1,i)}^*\|_F K_i\hat{d}(q)\leq KD(\mathcal{P})
\end{aligned}$$

$$K=\sum_{i=1}^{m}\sum_{l=1}^{i}\|G_{(l,i)}^*\|_F K_{(i,i-l)}^{(p^i,q)}+\sum_{i=1}^{m}\|G_{(1,i)}^*\|_F K_i$$

where $K_{(i,i-l)}^{(p^i,q)}$ is from lemma 7 and K_i is from Corollary 5.

Case 2: $q=\lambda$. First we show there exist constants $K_F^i > 0$, for $i \in \{1,\dots,m\}$ such that

$$\left\|\sum_{j=1}^{i}G_j^i-G_{(1,i)}^*\right\|_F \leq K_F^i D(\mathcal{P}). \qquad (55)$$

To do so, we use an analogous argument to the proof of [12, Lemma 2] with the following modifications:

We replace [12, Fact 1] with the following fact:

Fact: If there exist $k_{i,j}$ and d positive such that $|M_{i,j}| \leq k_{i,j}d$ for all i,j then there exists $K>0$ such that $\|M\|_F = \sqrt{\sum_{i,j}|M_{i,j}|^2} \leq Kd$.

Lemma 7 is used here in place of [12, Lemma 3] to establish [12, Corollary 2(a)].

Using (55), by an analogous argument to the proof of [12, Lemma 2] it follows that for all $l \in \{1,\dots,m_q\}$,

$$\left\|\hat{G}_l-\hat{G}_l^*\right\|_F \leq K_F^l D(\mathcal{P}).$$

Furthermore, the following inequality will be useful in deriving the error bounds.

$$\begin{aligned}
&\left\|\sum_{l=1}^{m_q}\left(\hat{G}_l-\hat{G}_l^*\right)\frac{1}{(s-q)^l}\right\|_{\mathcal{H}_2} \\
&\overset{\substack{\text{triangle}\\\text{inequality}}}{\leq}\sum_{l=1}^{m_q}\|\hat{G}_l-\hat{G}_l^*\|_F\sqrt{\frac{1}{2\pi}\int_{-\infty}^{\infty}\frac{1}{|j\omega-q|^{2l}}\mathrm{d}\omega} \qquad (56) \\
&\overset{\text{Lemma 2, 3}}{\leq}\sum_{l=1}^{m_q}K_F^l\sqrt{\frac{1}{\pi}}KD(\mathcal{P}).
\end{aligned}$$

Using the expressions for $\Phi_x(s)$ and $\Phi_x^*(s)$ from the proof of [12, Lemma 2], we compute

$$\begin{aligned}
&\|\Phi_x(s)-\Phi_x^*(s)\|_{\mathcal{H}_2} \\
&\leq\left\|\sum_{i=1}^{m_q+\tilde{m}}\tilde{G}_i\frac{1}{(s-q)^i}+\sum_{i=1+\tilde{m}}^{m}\sum_{j=1+\tilde{m}}^{m}G_j^i\frac{1}{(s-p_j^i)}\right. \\
&\left.-\sum_{i=1}^{m_q+m}\tilde{G}_i^*\frac{1}{(s-q)^i}\right\|_{\mathcal{H}_2}+\left\|\sum_{i=1}^{m_q}\left(\hat{G}_i-\hat{G}_i^*\right)\frac{1}{(s-q)^i}\right\|_{\mathcal{H}_2} \\
&\overset{(56)}{\leq}\left\|\sum_{i=1}^{m_q+\tilde{m}}\tilde{G}_i\frac{1}{(s-q)^i}+\sum_{i=1+\tilde{m}}^{m}\sum_{j=1+\tilde{m}}^{m}G_j^i\frac{1}{(s-p_j^i)}\right. \\
&\left.-\sum_{i=1}^{m_q+m}\tilde{G}_i^*\frac{1}{(s-q)^i}\right\|_{\mathcal{H}_2}+\sum_{i=1}^{m_q}K_F^i\sqrt{\frac{1}{\pi}}KD(\mathcal{P}).
\end{aligned}$$

For the remainder of the proof let Φ_x and Φ_x^* denote $\sum_{i=1}^{m_q+\tilde{m}} \tilde{G}_i \frac{1}{(s-q)^i} + \sum_{i=1+\tilde{m}}^{m} \sum_{j=1+\tilde{m}}^{m} G_j^i \frac{1}{(s-p_j^i)}$ and $\sum_{i=1}^{m_q+m} \tilde{G}_i^* \frac{1}{(s-q)^i}$, respectively. It suffices to show that there exists $K > 0$ such that the first term is bounded in terms of $D(\mathcal{P})$, i.e., the redefined $\|\Phi_x(s) - \Phi_x^*(s)\|_{\mathcal{H}_2} \leq KD(\mathcal{P})$. We use the following fact:

Fact: If there exist $k_{i,j} > 0$ and D such that $\|M_{i,j}(s)\|_{\mathcal{H}_2} \leq k_{i,j}D$ for all i, j then there exists $K > 0$ such that $\|M(s)\|_{\mathcal{H}_2} \leq KD$.

By the proof of [12, Lemma 2], to evaluate $\|\Phi_x(s) - \Phi_x^*(s)\|_{\mathcal{H}_2}$, it suffices to consider the lth superdiagonal of the term multiplying BH_i^* in $\Phi_x(s) - \Phi_x^*(s)$. For $i \in \{1 + \tilde{m}, \dots, m\}$ and $l \in \{m_q - i, \dots, m_q - 2\}$, this is given by

$$\left\| \frac{(s-q)^{-(l+1+\tilde{m})}}{\prod_{j=1+\tilde{m}}^{i}(s-p_j^i)} - \frac{1}{(s-q)^{i+l+1}} \right\|_{\mathcal{H}_2} \overset{\text{Lemma 7}}{\leq} k_{i,l}\hat{d}(q). \tag{57}$$

for some $k_{i,l} > 0$ and for $i \in \{1+\tilde{m}, \dots, m\}$, the (m_q-1)th superdiagonal (i.e. $l = m_q - 1$) of the term multiplying BH_i^* in $\Phi_x(s) - \Phi_x^*(s)$ is

$$\left\| \frac{1}{(s-q)^{l+1}} \frac{1}{\prod_{j=1}^{i}(s-p_j^i)} - \frac{1}{(s-q)^{i+l+1}} \right\|_{\mathcal{H}_2} \overset{\text{Lemma 7}}{\leq} k_{i,l}\hat{d}(q).$$

for some $k_{i,l} > 0$ and for $i \in \{1 + \tilde{m}, \dots, m\}$ and $l \in \{0, \dots, m_q - i - 1\}$, the lth superdiagonal of the term multiplying BH_i^* in $\Phi_x(s) - \Phi_x^*(s)$ is the same bound in (57).

Finally, if $\tilde{m} = 1$, then for $i = 1$ and any $l \in \{0, \dots, m_q - 1\}$, the lth superdiagonal of the term multiplying BH_1^* in $\Phi_x(s) - \Phi_x^*(s)$ is 0. Thus, by the fact there exists $K > 0$ such that

$$\|\Phi_x(s) - \Phi_x^*(s)\|_{\mathcal{H}_2} \leq KD(\mathcal{P}). \tag{58}$$

The argument that $\|\Phi_x(s) - \Phi_x^*(s)\|_{\mathcal{H}_\infty} \leq KD(\mathcal{P})$ is analogous to the argument for the discrete time setting in the proof of [12, Lemma 2] except that Lemma 7 is used here in place of [12, Lemma 3]. Combining this and (58) proves Lemma 6. □

Proof of Theorem 5 and Corollary 2: The proofs follow analogous arguments to the proofs of [12, Theorem 1 and Corollary 1]. □

VIII. Conclusion

In this paper, a new Galerkin-type method for finite dimensional approximations of transfer functions in continuous time Hardy space by a selection of simple poles (SPA) was developed. For any transfer function in Hardy space, approximation error bounds for SPA were provided which bound the $\mathcal{H}_2$ and $\mathcal{H}_\infty$ norms between the SPA and that transfer function, and are proportional to the geometric distance between their poles. These were then used to show that for any arbitrary compact set and any space-filling sequence of poles within it, the space of SPAs converges to the subset of Hardy space consisting of transfer functions whose poles all lie within that compact set. Furthermore, a uniform convergence rate was provided that depends purely on the geometry of the SPA pole selection, and this was specialized for a particularly interesting selection proposed based on a grid overlaid on a trapezoid.

Then, SLS with continuous time SPA was used to develop the first tractable approach for mixed $\mathcal{H}_2/\mathcal{H}_\infty$ control design in continuous time with SLS. The proposed formulation results in a convex and tractable SDP for the control design consisting of LMIs and affine constraints, which can be solved efficiently. A general suboptimality certificate was provided for the proposed control design method that converges to the ground-truth optimal solution of the infinite dimensional design problem as the number of poles approaches infinity, with a uniform convergence rate that depends purely on the geometry of the pole selection. Then, this general suboptimality bound was specialized to the particularly interesting case of the proposed trapezoidal grid pole selection strategy, and a uniform convergence rate was provided for this pole selection. A numerical example of frequency and voltage regulation by a wind turbine interfaced to the power grid via a power converter showed that the proposed control design method achieved close matching with the desired closed-loop behavior with only a small number of poles.

References

[1] D. S. Bernstein and W. M. Haddad, "Lqg control with an $\mathcal{H}_\infty$ performance bound: A riccati equation approach," in *1988 American Control Conference*, pp. 796–802, 1988.

[2] Y. Du and J. S. Li, "Distributed continuous-time control via system level synthesis," 2025.

[3] Y. Zheng, L. Furieri, A. Papachristodoulou, N. Li, and M. Kamgarpour, "On the equivalence of youla, system-level, and input–output parameterizations," *IEEE Transactions on Automatic Control*, vol. 66, no. 1, pp. 413–420, 2020.

[4] D. Youla, H. Jabr, and J. Bongiorno, "Modern wiener-hopf design of optimal controllers–part ii: The multivariable case," *IEEE Transactions on Automatic Control*, vol. 21, no. 3, pp. 319–338, 1976.

[5] J. Anderson, J. C. Doyle, S. H. Low, and N. Matni, "System level synthesis," *Annual Reviews in Control*, vol. 47, pp. 364–393, 2019.

[6] L. Furieri, Y. Zheng, A. Papachristodoulou, and M. Kamgarpour, "An input–output parametrization of stabilizing controllers: Amidst youla and system level synthesis," *IEEE Control Systems Letters*, vol. 3, no. 4, pp. 1014–1019, 2019.

[7] L. Lessard and S. Lall, "An algebraic approach to the control of decentralized systems," *IEEE Transactions on Control of Network Systems*, vol. 1, no. 4, pp. 308–317, 2014.

[8] J. S. L. Li and J. C. Doyle, "Distributed robust control for systems with structured uncertainties," in *2022 IEEE 61st Conference on Decision and Control (CDC)*, pp. 1702–1707, 2022.

[9] J. Yu, Y.-S. Wang, and J. Anderson, "Localized and distributed $\mathcal{H}_2$ state feedback control," in *2021 American Control Conference (ACC)*, pp. 2732–2738, IEEE, 2021.

[10] J. S. Li, C. A. Alonso, and J. C. Doyle, "Frontiers in scalable distributed control: Sls, mpc, and beyond," in *2021 American Control Conference (ACC)*, pp. 2720–2725, IEEE, 2021.

[11] M. W. Fisher, G. Hug, and F. Dörfler, "Approximation by simple poles—part i: Density and geometric convergence rate in hardy space," *IEEE Transactions on Automatic Control*, vol. 69, no. 8, pp. 4894–4909, 2024.

[12] M. W. Fisher, G. Hug, and F. Dörfler, "Approximation by simple poles—part ii: System level synthesis beyond finite impulse response," *IEEE Transactions on Automatic Control*, vol. 70, no. 3, pp. 1411–1426, 2025.

[13] Z. Fang and M. W. Fisher, "Hybrid state space and frequency domain system level synthesis for sparsity-promoting $\mathcal{H}_2/\mathcal{H}_\infty$ control design," in *2024 IEEE 63rd Conference on Decision and Control (CDC)*, pp. 8473–8478, 2024.

[14] O. Kjellqvist and J. Yu, "On infinite-horizon system level synthesis problems," in *2022 IEEE 61st Conference on Decision and Control (CDC)*, pp. 5238–5244, IEEE, 2022.

[15] A. C. Antoulas, *Approximation of Large-Scale Dynamical Systems*. SIAM, 2005.

[16] J. Doyle, "Robust and optimal control," in *Proceedings of 35th IEEE Conference on Decision and Control*, vol. 2, pp. 1595–1598, 1996.

[17] P. Frey and P. George, "Mesh generation: Application to finite elements: Second edition," *Mesh Generation: Application to Finite Elements: Second Edition*, 01 2008.

[18] C. Scherer and S. Weiland, "Linear matrix inequalities in control," *Lecture Notes, Dutch Institute for Systems and Control, Delft, The Netherlands*, vol. 3, no. 2, 2000.

[19] E. D. Andersen and K. D. Andersen, "The mosek interior point optimizer for linear programming: an implementation of the homogeneous algorithm," in *High performance optimization*, pp. 197–232, Springer, 2000.

[20] J. Lofberg, "Yalmip: A toolbox for modeling and optimization in matlab," in *2004 IEEE international conference on robotics and automation (IEEE Cat. No. 04CH37508)*, pp. 284–289, 2004.

[21] A. Jeffrey and D. Zwillinger, *Table of integrals, series, and products*. Elsevier Science, 2007.

[22] V. V. Prasolov, *Polynomials*, vol. 11. Springer Science & Business Media, 2009.

Zhong Fang received his M.A.Sc. in Electrical and Computer Engineering from the University of Waterloo in 2025 and his B.Sc. in Applied Mathematics from Wuhan University in 2023.

His research interests include control theory, optimization, and cyber-physical systems.

Michael W. Fisher is an Assistant Professor in the Department of Electrical and Computer Engineering at the University of Waterloo, Canada. He was a postdoctoral researcher with the Automatic Control and Power System Laboratories at ETH Zurich. He received his Ph.D. in Electrical Engineering: Systems at the University of Michigan, Ann Arbor in 2020, and a M.Sc. in Mathematics from the same institution in 2017. He received his B.A. in Mathematics and Physics from Swarthmore College in 2014. His research interests are in dynamics, control, and optimization of complex systems, with an emphasis on electric power systems. He was a finalist for the 2017 Conference on Decision and Control (CDC) Best Student Paper Award and a recipient of the 2019 CDC Outstanding Student Paper Award.